UNIVERSITY of CALIFORNIA
Santa Barbara

AVERAGING ALGORITHMS AND COVERAGE CONTROL

A Thesis submitted in partial satisfaction of the
requirements for the degree

Master of Science
in
Mechanical Engineering

by

Chunkai Gao

Committee in charge:

Professor Francesco Bullo, Chair
Professor João Hespanha
Professor Bassam Bamieh

September 2007

The thesis of Chunkai Gao is approved.

Professor João Hespanha

Professor Bassam Bamieh

Professor Francesco Bullo, Committee Chair

September 2007

AVERAGING ALGORITHMS AND COVERAGE CONTROL

by

Chunkai Gao

Acknowledgements

First of all, I would like to express my sincere gratitude to my advisor, Prof. Francesco Bullo, for his guidance and assistance over the past two and half years. He has not only been a great mentor but also a good friend to me.

I would also like to acknowledge Prof. João Hespanha for his great classroom teaching. Four of my control-related courses are taken with him, which became the foundations of my understanding of this area.

Thanks also to Prof. Jorge Cortés and Prof. Ali Jadbabaie for their collaboration and advice on my research.

I thank Prof. Bassam Bamieh for being in my thesis committee, and Prof. Brad Paden for giving me suggestions on graduate study.

I thank Laura Reynolds for her kind and immediate help in administrative issues.

Lastly, I am thankful to my lab-mates, Sonia, Anurag, Ketan, Sara, Giuseppe, Stephen, Karl, Shaunak and Kurt, for their great help both in and out of the lab, professionally and socially.

Abstract

AVERAGING ALGORITHMS AND COVERAGE CONTROL

by

Chunkai Gao

This thesis summarizes our work on averaging algorithms, dynamic consensus and coverage control.

In the first part of this thesis, we show the relationship between two algorithms and optimization problems that are the subject of recent attention in the networking and control literature. First, we obtain some results on averaging algorithms over acyclic digraphs with fixed and controlled-switching topology. Second, we discuss continuous and discrete coverage control laws. Further, we show how discrete coverage control laws can be cast as averaging algorithms defined over an appropriate graph that we term the discrete Voronoi graph.

In the second part of this thesis, we study dynamic consensus algorithms and their applications for multi-agent coordination. First, we propose a dynamic max-consensus estimator based on the concept of dynamic average consensus and static max-consensus. Second, we discuss how to design distributed control laws to optimize coverage performance globally under the distributed estimation-and-control framework. Various numerical simulations verify the effectiveness of our results.

Contents

List of Figures

Chapter 1

Introduction

Consensus and coverage control are two distinct problems within the recent literature on multi-agent coordination and cooperative robotics. Both problems have attracted much attention among researchers studying distributed and decentralized systems. Roughly speaking, the objective of the consensus problem is to analyze and design scalable distributed control laws to drive the groups of agents to agree upon certain quantities of interest. On the other hand, the objective of the coverage control problem is to deploy the agents to get optimal sensing performance of an environment of interest. The main result of the paper shows the relationship between averaging over switching acyclic digraphs and discrete coverage. Various simulations illustrate this result, and show the consistent parallelism between the continuous and the discrete settings.

The thesis is organized as follows. Firstly, for the reader's convenience, we review some basic mathematical notions and tools that will be commonly

used in this thesis in Chapter 2, including Voronoi diagrams, graph theory, Filippov solutions and non-smooth analysis. In Chapter 3, we investigate the properties of averaging algorithms over acyclic digraphs with fixed and controlled-switching topologies. In Chapter 4, we first review the multi-center optimization problem and the corresponding coverage control algorithm. We then study the multi-center optimization problem in discrete space and derive a discrete coverage control law. Finally, we show that the discrete coverage control law is an averaging algorithm over a certain set of acyclic digraphs. Chapter 3 and Chapter 4 form the first part of the thesis. In Chapter 5, we first review the concept and properties of proportional dynamic average consensus estimator; then we propose a dynamic maximum consensus estimator and verify its effectiveness by simulations. In Chapter 6, we first introduce a deterministic global optimization scheme named Terminal Repeller Unconstrained Subenergy Tunneling (TRUST); then we discuss the distributed estimation and control approach to solve global optimal coverage problem and report the numerical simulation results. Chapter 5 and Chapter 6 form the second part of this thesis.

Chapter 2

Mathematical Preliminaries

For the reader's convenience, this chapter presents some basic mathematical notions and tools that will be commonly used in this thesis. Since the space is limited, the discussions may not be in full detail. The reader who wishes to understand the materials covered in this chapter with full formal derivations should consult the relevant books, such as Okabe, Boots, Sugihara and Chiu's book [2] on Voronoi diagrams; Diestel's book [3] on graph theory; Filippov's book [4] on discontinuous dynamical systems; Clarke's book [5] on nonsmooth analysis; and Bacciotti and Rosier's book [6] on Lyapunov functions and stability theory.

Notation

Let $\mathbb{N}$ denote the set of natural numbers. Let $\mathbb{R}$, $\mathbb{R}_{\geq 0}$ and $\mathbb{R}_{>0}$ denote, respectively, the set of real, non-negative real and positive real numbers. For any set $\mathcal{S} \subseteq \mathbb{R}^2$, we let $\overset{\circ}{\mathcal{S}}$, and $\partial\mathcal{S}$ denote, respectively, the interior, and boundary of

S. The quadratic form associated with a symmetric matrix $B \in \mathbb{R}^{n\times n}$ is the function defined by $x \mapsto x^T Bx$. The map $f : X \to Y$ and the set-valued map $f : X \rightrightarrows Y$ associate to a point in X a point in Y and a subset of Y, respectively. The sum of m subsets $S_i, i \in \{1, \ldots, m\}$ in a vector space, denoted by $\sum_{i=1}^{m} S_i$, consists of all vectors of the form $\sum_{i=1}^{m} s_i$, where $s_i \in S_i$, for $i \in \{1, \ldots, m\}$.

2.1 Voronoi Diagrams

The concept of Voronoi diagrams is widely used in coverage control and other locational optimization problems. It has been rediscovered independently in different fields for many times [2]. In Section 2.1.1, we introduce the basic definition of (ordinary) Voronoi diagram, and in Section 2.1.2, we introduce the concept of generalized Voronoi diagram.

2.1.1 Ordinary Voronoi Diagram

Suppose we have a finite number, $n \in [2, \infty)$, of points, $(p_1, \ldots, p_n)$, in $\mathbb{R}^m$, where $m \in \mathbb{N}$. These n points have location vectors $x_1, \ldots, x_n$, respectively. Let p be an arbitrary point in $\mathbb{R}^m$ with location vector x. Define the index set $I_n = \{1, 2, \ldots, n\}$, then we have the following definition of Voromoi diagram.

Definition 2.1.1 (Voronoi diagram in $\mathbb{R}^m$ [2]). *Let ($P = \{p_1, \ldots, p_n\}$, where $2 \leq n < \infty$ and $p_i \in \mathbb{R}^m$, $x_i \neq x_j$, for $i \neq j$, $i, j \in I_n$. We call the region given by*

$$V(p_i) = \{x \mid \|x - x_i\| \leq \|x - x_j\|, \text{for } j \neq i, j \in I_n\} \tag{2.1}$$

the m-dimensional Voronoi polyhedron *associated with p_i, and the set $\mathcal{V}(P) =$*

$\{V(p_1), \ldots, V(p_n)\}$ *the m-dimensional Voronoi diagram generated by* P.

An example Voronoi diagram in $\mathbb{R}^2$ is shown in Figure 2.1, where we consider a polygon in $\mathbb{R}^2$ with 8 generator points, $P = \{p_1, \ldots, p_8\}$. The assigned region $V(p_i)$, for $i \in \{1, \ldots, 8\}$, is the shaded area where point p_i sits in.

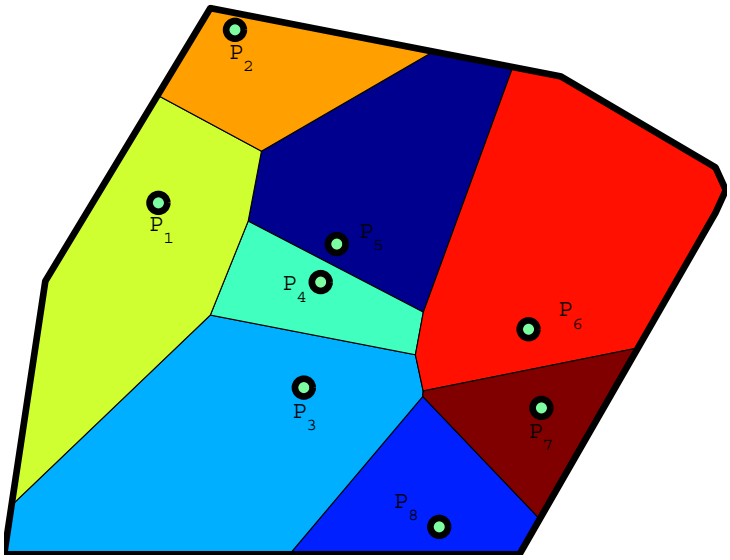

Figure 2.1: A planar Voronoi diagram.

2.1.2 Weighted Voronoi Diagram

We notice from definition 2.1.1 that the core idea for defining Voronoi diagram is that every point in a space is assigned to at least one of the generators with shortest Euclidean distance from this point. By extending the assignment rule, Voronoi diagram can be generalized in a variety of ways. Formal

mathematical approach of generalized Voronoi diagram is available in [2]. To save space, we will cover only one kind of very specific generalized Voronoi diagrams, namely weighted Voronoi diagram, which is used widely in many fields.

In the definition of Voronoi diagram, we implicitly assume that all the generator points have the same weight. While in some practical scenarios, this assumption may not be appropriate. Rather, it is more appropriate to assume that generators have different weights according to the variable property or ability of the generators. For example, in sensor networks we may have sensors with different sensing ability.

As same as in Section 2.1.1, we consider a set of n distinct points, $P = \{p_1, \ldots, p_n\}$, in $\mathbb{R}^m$. Each p_i has weight w_i, which is assigned according to the different properties of the generator points. In applications, w_i could be a number, a vector, or some other parameter. With this weight, we denote the *weighted distance* from any point $p \in \mathbb{R}^m$ to p_i as $d_w(p, p_i)$, which needs to be specified properly in applications. For any $i, j \in \{1, \ldots, n\}$ and $j \neq i$, the dominance region of p_i over p_j with the weighted distance is defined as

$$\mathrm{Dom}(p_i, p_j) = \{p \in \mathbb{R}^m \mid d_w(p, p_i) \leq d_w(p, p_j)\}. \tag{2.2}$$

Let

$$V(p_i) = \bigcap_{j \in I_n, j \neq i} \mathrm{Dom}(p_i, p_j).$$

If the dominance region is well defined in (2.2), then $\mathcal{V}(P, W) = \{V(p_i), \ldots, V(p_n)\}$, where $W = (w_i, \ldots, w_n)$, defines a *weighted Voronoi diagram* generated by P with weight W, and the set $V(p_i)$ is the *weighted Voronoi region* associated with p_i. Since the weighted distance d_w can be defined differently, many differ-

ent kinds of weighted Voronoi diagrams are possible, such as multiplicatively weighted Voronoi diagram with distance function d_{mw} defined as

$$d_{mw}(p, p_i) = \frac{1}{w_i}\|x - x_i\|, \quad w_i > 0,$$

and additively weighted Voronoi diagram with distance function d_{aw} defined as

$$d_{aw}(p, p_i) = \|x - x_i\| - w_i, \quad w_i \in \mathbb{R}.$$

The properties of these two kinds of weighted Voronoi diagrams are discussed extensively in [2].

2.2 Graph theory

In mathematics and computer science, graphs are mathematical structures used to model pairwise relations between objects from a certain collection, and graph theory is the study of graphs. A graph may be undirected, meaning that there is no distinction between the two vertices associated with each edge, or its edges may be directed from one vertex to another. The edges of a graph may be have different weights. A weighted graph associates a label, called *weight*, with every edge in the graph. Weights are usually real numbers. They may be restricted to rational numbers or integers. Certain algorithms require further restrictions on weights. Sometimes a non-edge is labeled by a special weight representing zero (Eg. when considering capacity of direct communication between two nodes) or infinity (Eg. when considering length of direct path between two nodes). In this thesis, we assign a non-edge weight 0 in the following chapters.

Mathematically speaking, a *graph* or *undirected graph* is an ordered pair $\mathcal{G} = (\mathcal{U}, \mathcal{E})$ of sets satisfying $\mathcal{E} \in 2^{\mathcal{U}\times\mathcal{U}}$ (recall that $2^{\mathcal{U}}$ is the collection of subsets of $\mathcal{U}$). The elements of $\mathcal{U}$ are the *vertices* (or *notes*) of the graph $\mathcal{G}$, the elements of $\mathcal{E}$ are its *edges*. The number of vertices of a graph $\mathcal{G}$ is its *order*. Two vertices of $\mathcal{G}$ are *adjacent*, or *neighbors*, if there is an edge between these two vertices.

A *weighted directed graph*, in short *digraph*, $\mathcal{G} = (\mathcal{U}, \mathcal{E}, \mathcal{A})$ of order n consists of a vertex set $\mathcal{U}$ with n elements, an edge set $\mathcal{E} \in 2^{\mathcal{U}\times\mathcal{U}}$, and a *weighted adjacency matrix* $\mathcal{A}$ with nonnegative entries a_{ij}, $i, j \in \{1, \ldots, n\}$. For simplicity, we take $\mathcal{U} = \{1, \ldots, n\}$. For $i, j \in \{1, \ldots, n\}$, the entry a_{ij} is positive if and only if the pair (i, j) is an edge of $\mathcal{G}$, i.e., $a_{ij} > 0 \Leftrightarrow (i, j) \in \mathcal{E}$. We also assume $a_{ii} = 0$ for all $i \in \{1, \ldots, n\}$ and $a_{ij} = 0$ if $(i, j) \notin \mathcal{E}$, for all $i, j \in \{1, \ldots, n\}$ and $i \neq j$. When convenient, we will refer to the adjacency matrix of $\mathcal{G}$ by $\mathcal{A}(\mathcal{G})$.

Weighted digraphs are used extensively in the following chapters. Let us now review some basic connectivity notions for digraphs. A *directed path* in a digraph is an ordered sequence of vertices such that any two consecutive vertices in the sequence are an edge of the digraph. A *cycle* is a non-trivial directed path that starts and ends at the same vertex. A digraph is *acyclic* if it contains no directed cycles. A node of a digraph is *globally reachable* if it can be reached from any other node by traversing a directed path. A digraph is *strongly connected* if every node is globally reachable.

Remark 2.2.1. *The previous definition of adjacency matrix follows the convention adopted in [7], where $a_{ij} > 0 \Leftrightarrow (i, j) \in \mathcal{E}$. On the other hand, in [8], $a_{ij} > 0 \Leftrightarrow (j, i) \in \mathcal{E}$. This difference arises from a different meaning of the direction of an edge. In [7], a directed edge $(i, j) \in \mathcal{E}$ means node i can 'see' node j, i.e., node i can*

obtain, in some way, information from node j. We refer to this as the communication *interpretation. In [8], a directed edge $(i, j) \in \mathcal{E}$ means that the information of node i can flow to node j. We refer to this as the* sensing *interpretation. The difference leads to different statements of various results. For example, having a globally reachable node in the communication interpretation is equivalent to having a spanning tree in the sensing interpretation.* •

The *out-degree* and the *in-degree* of node i are defined by, respectively,

$$d_{\text{out}}(i) = \sum_{j=1}^{n} a_{ij}, \quad d_{\text{in}}(i) = \sum_{j=1}^{n} a_{ji}.$$

The out-degree matrix $D_{\text{out}}(\mathcal{G})$ and the in-degree matrix $D_{\text{in}}(\mathcal{G})$ are the diagonal matrices defined by $(D_{\text{out}}(\mathcal{G}))_{ii} = d_{\text{out}}(i)$ and $(D_{\text{in}}(\mathcal{G}))_{ii} = d_{\text{in}}(i)$, respectively. The digraph $\mathcal{G}$ is *balanced* if $D_{\text{out}}(\mathcal{G}) = D_{\text{in}}(\mathcal{G})$. The *graph Laplacian* of the digraph $\mathcal{G}$ is

$$L(\mathcal{G}) = D_{\text{out}}(\mathcal{G}) - \mathcal{A}(\mathcal{G}),$$

or, in components,

$$l_{ij}(\mathcal{G}) = \begin{cases} \sum_{k=1, k\neq i}^{n} a_{ik}, & j = i, \\ -a_{ij}, & j \neq i. \end{cases}$$

Next, we define reverse and mirror digraphs. Let $\tilde{\mathcal{E}}$ be the set of reverse edges of $\mathcal{G}$ obtained by reversing the order of all the pairs in $\mathcal{E}$. The *reverse digraph* of $\mathcal{G}$, denoted $\tilde{\mathcal{G}}$, is $(\mathcal{U}, \tilde{\mathcal{E}}, \tilde{\mathcal{A}})$, where $\tilde{\mathcal{A}} = \mathcal{A}^T$. The *mirror digraph* of $\mathcal{G}$, denoted $\hat{\mathcal{G}}$, is $(\mathcal{U}, \hat{\mathcal{E}}, \hat{\mathcal{A}})$, where $\hat{\mathcal{E}} = \mathcal{E} \cup \tilde{\mathcal{E}}$ and $\hat{\mathcal{A}} = (\mathcal{A} + \mathcal{A}^T)/2$. Note that $L(\tilde{\mathcal{G}}) = D_{\text{out}}(\tilde{\mathcal{G}}) - \mathcal{A}(\tilde{\mathcal{G}}) = D_{\text{in}}(\mathcal{G}) - \mathcal{A}(\mathcal{G})^T$.

2.3 Filippov solutions for discontinuous dynamical systems

In this section, we consider dynamical systems of the following general form

$$\dot{x}(t) = X(t, x(t)), \tag{2.3}$$

with state vector $x \in \mathbb{R}^m$, $m \in \mathbb{N}$, and vector field $X : \mathbb{R} \times \mathbb{R}^m \to \mathbb{R}^m$. By discontinuous dynamical system we mean that the vector field X can be a discontinuous function of the state x, i.e., for any fixed $t \in \mathbb{R}$, $X(t, x)$, as a function of x, is not necessarily continuous. Discontinuous dynamical systems exist in may control applications, such as optimal control and sliding mode control. Since the vector field is discontinuous, continuously differentiable curves that satisfy the associated dynamical system do not exist in general, which motivates the need of identifying a suitable notion of solution. To solve this problem, several different notions have been developed in the literature, such as Caratheodory and Filippov solutions. By allowing classical solutions not to follow the direction of the vector field at a few time instants, Caratheodory solutions give the most natural generalization of the classical notion of solution. However, this relaxation is still too rigid to cope with the discontinuity [9], and Caratheodory solutions do not exist in many practical applications. On the other hand, Filippov solutions make use of the concept of differential inclusion, which gives more flexibility in the notion of solutions. For this reason, We adopt the notion of Filippov solutions to analysis discontinuous dynamical system in the following chapters of the thesis. Before we introduce the formal definition of Filippov solutions, we bring to the reader's attention that a tutorial of notions

of solutions is presented in [9].

For vector field $X : \mathbb{R} \times \mathbb{R}^m \to \mathbb{R}^m$, we define Filippov set-valued map $K[X] : \mathbb{R} \times \mathbb{R}^m \to 2^{\mathbb{R}^m}$ as

$$K[X](t,x) = \bigcap_{\delta>0} \bigcap_{\mu(S)=0} \mathrm{co}\{X(t, B(x,\delta) \setminus S)\},$$

where operator co denotes convex closure, μ denotes the Lebesgue measure, and $B(x,\delta)$ denotes a ball centered at x with radius δ. Substitute the differential equation (2.3) by the following differential inclusion

$$\dot{x}(t) \in K[X](t, x(t)). \tag{2.4}$$

A *Filippov solution* of (2.3), defined on $[t_0, t_1] \subset \mathbb{R}$, is a solution of the differential inclusion (2.4), that is, an absolutely continuous function $\gamma : [t_0, t_1] \to \mathbb{R}^m$ such that $\dot{\gamma}(t) \in K[X](t, \gamma(t))$ for almost every $t \in [t_0, t_1]$. The next result, adopted from [9], establishes conditions under which Filippov solutions exist.

Proposition 2.3.1 (Existence of Filippov solutions)**.** *For $X : \mathbb{R} \times \mathbb{R}^m \to \mathbb{R}^m$ measurable and locally essentially bounded, there exists at least one Filippov solution of* (2.3) *starting from any initial condition.*

Besides existence of Filippov solutions, another basic problem is the uniqueness. In general, discontinuous dynamical systems do not have unique Filippov solutions. The next result, adopted from [4], provides one result about uniqueness of Filippov solutions.

Proposition 2.3.2 (Uniqueness of Filippov solutions)**.** *Let $X : \mathbb{R} \times \mathbb{R}^m \to \mathbb{R}^m$ measurable and locally essentially bounded. Assume that for all $(t,x) \in \mathbb{R} \times \mathbb{R}^m$, there exists $L_X(t)$ and $\varepsilon \in (0,\infty)$, such that for every y, $y' \in B(x,\varepsilon)$, one has*

$$(X(t,y) - X(t,y'))^T (y - y') \leq L_X(t) \|y - y'\|_2^2. \tag{2.5}$$

Assume that function $L_X : \mathbb{R} \to \mathbb{R}$ *is integrable, then, for any* $(t_0, x_0) \in \mathbb{R} \times \mathbb{R}^m$, *there exists a unique Filippov solution of* (2.3) *with initial condition* $x(t_0) = x_0$.

2.4 Basic ideas and calculus of generalized gradient

The generalized gradient is a replacement for the derivative. Given a locally Lipschitz function $f : \mathbb{R}^M \to \mathbb{R}$, let Ω_f be the set of points in $\mathbb{R}^M$ at which f fails to be differentiable, and let S be any other set of measure zero, then the generalized gradient $\partial f : \mathbb{R}^M \to 2^{\mathbb{R}^M}$ of f is defined as

$$\partial f(x) = \text{co}\{\lim_{i \to \infty} \nabla f(x_i) \mid x_i \to x, x_i \notin S \cup \Omega_f\},$$

which says that $\partial f(x)$ is the convex combination of all points of the form $\lim \nabla f(x_i)$, where $\{x_i\}$ is any sequence which converges to x while avoiding $S \cup \Omega_f$. It is easy to see that when f is continuously differentiable at x, $\partial f(x)$ reduces to the singleton set $\{\nabla f(x)\}$.

In general, the computation of $\partial f(x)$ from the definition is difficult. Researchers have developed basic calculus of generalized gradient of functions to simplify this calculation. In the rest part of this section we review some properties in this basic calculus of generalized gradient presented in [5].

Proposition 2.4.1 (Scalar multiples)**.** *If* $f : \mathbb{R}^M \to \mathbb{R}$ *is locally Lipschitz at* $x \in \mathbb{R}^M$, *then, for any scalar* s, sf *is locally Lipschitz at* x *and*

$$\partial(sf)(x) = s\partial f(x).$$

Proposition 2.4.2 (Finite sums)**.** *If* $f_i : \mathbb{R}^M \to \mathbb{R}$, $i \in \{1, \ldots, m\}$, *are locally Lipschitz at* $x \in \mathbb{R}^M$, *then, for any scalars* $\{s_1, \ldots, s_m\}$, $\sum_{i=1}^m s_i f_i$ *is locally Lipschitz*

and

$$\partial\Big(\sum_{i=1}^{m} s_i f_i\Big)(x) \subset \sum_{i=1}^{m} s_i \partial f_i(x),$$

where equality holds if each f_i is regular at x and each s_i is nonnegative.

Proposition 2.4.3 (Chain Rule)**.** *Let F be a map from X to another Banach space Y, and let g be a real-valued function on Y. Suppose that F is strictly differentiable at x and that g is Lipschitz near $F(x)$. Then, $f = g \circ F$ is Lipschitz near x, and one has*

$$\partial f(x) \subset \partial g(F(x)) \circ D_s F(x),$$

and equality holds if g (or $-g$) is regular at $F(x)$, in which case f (or $-f$) is also regular at x.

Proposition 2.4.4. *Let $f_k : \mathbb{R}^M \to \mathbb{R}$, $k \in \{1, \ldots, m\}$ be locally Lipschitz functions at $x \in \mathbb{R}^M$ and let $f(x') = \max\{f_k(x') \mid k \in \{1, \ldots, m\}\}$. Then,*

(i) f is locally Lipschitz at x,

(ii) if $I(x')$ denotes the set of indexes k for which $f_k(x') = f(x')$, we have

$$\partial f(x) \subset \operatorname{co}\{\partial f_i(x) \mid i \in I(x)\},$$

and if f_i, $i \in I(x)$, is regular at x, then equality holds and f is regular at x.

2.5 Stability analysis via nonsmooth Lyapunov functions

Throughout the thesis, as mentioned in section 2.3, we define the solutions of differential equations with discontinuous right-hand sides in terms of differ-

ential inclusions. In section 2.3, we introduced the notion of Filippov solution of dynamical system (2.3), and results on its existence and uniqueness. Instead of talking about general non-autonomous dynamical system (2.3), we focus on more special autonomous dynamical system in this section. Let $F : \mathbb{R}^N \to 2^{\mathbb{R}^N}$ be a set-valued map. Consider the differential inclusion

$$\dot{x} \in F(x)\,. \tag{2.6}$$

A solution to this equation on an interval $[t_0, t_1] \subset \mathbb{R}$ is defined as an absolutely continuous function $x : [t_0, t_1] \to \mathbb{R}^N$ such that $\dot{x}(t) \in F(x(t))$ for almost all $t \in [t_0, t_1]$. Given $x_0 \in \mathbb{R}^N$, the existence of at least a solution with initial condition x_0 is guaranteed by the following lemma.

Lemma 2.5.1. *Let the mapping F be upper semicontinuous with nonempty, compact and convex values. Then, given $x_0 \in \mathbb{R}^N$, there exists a local solution of* (2.6) *with initial condition x_0.*

Now, consider the differential equation

$$\dot{x}(t) = X(x(t))\,, \tag{2.7}$$

where $X : \mathbb{R}^N \to \mathbb{R}^N$ is measurable and essentially locally bounded. Here, we understand the solution of this equation in the Filippov sense. For each $x \in \mathbb{R}^N$, consider the set

$$K[X](x) = \bigcap_{\delta>0} \bigcap_{\mu(S)=0} \mathrm{co}\{X(B_N(x,\delta) \setminus S)\}\,.$$

Alternatively, one can show [10] that there exists a set S_X of measure zero such that

$$K[X](x) = \mathrm{co}\{\lim_{i\to+\infty} X(x_i) \mid x_i \to x\,,\ x_i \notin S \cup S_X\}\,,$$

where S is any set of measure zero. A Filippov solution of (2.7) on an interval $[t_0, t_1] \subset \mathbb{R}$ is defined as a solution of the differential inclusion $\dot{x} \in K[X](x)$. Since the multivalued mapping $K[X] : \mathbb{R}^N \to 2^{\mathbb{R}^N}$ is upper semicontinuous with nonempty, compact, convex values and locally bounded (cf. [4]), the existence of Filippov solutions of (2.7) is guaranteed by Lemma 2.5.1.

Given a locally Lipschitz function $f : \mathbb{R}^N \to \mathbb{R}$, the *set-valued Lie derivative of f with respect to X* at x is defined as

$$\tilde{\mathcal{L}}_X f(x) = \{a \in \mathbb{R} \mid \exists v \in K[X](x) \text{ such that } \zeta \cdot v = a\,,\ \forall \zeta \in \partial f(x)\}\,.$$

For each $x \in \mathbb{R}^N$, $\tilde{\mathcal{L}}_X f(x)$ is a closed and bounded interval in $\mathbb{R}$, possibly empty. If f is continuously differentiable at x, then $\tilde{\mathcal{L}}_X f(x) = \{df \cdot v \mid v \in K[X](x)\}$. If, in addition, X is continuous at x, then $\tilde{\mathcal{L}}_X f(x)$ corresponds to the singleton $\{\mathcal{L}_X f(x)\}$, the usual Lie derivative of f in the direction of X at x.

The following result is a generalization of LaSalle Invariance Principle for differential equations of the form (2.7) with nonsmooth Lyapunov functions. The formulation is taken from [11], and slightly generalizes the one presented in [12].

Theorem 2.5.2 (LaSalle principle)**.** *Let $f : \mathbb{R}^N \to \mathbb{R}$ be a locally Lipschitz and regular function. Let $x_0 \in \mathbb{R}^N$ and let $f^{-1}(\leq f(x_0), x_0)$ be the connected component of $\{x \in \mathbb{R}^N \mid f(x) \leq f(x_0)\}$ containing x_0. Assume the set $f^{-1}(\leq f(x_0), x_0)$ is bounded and assume either $\max \tilde{\mathcal{L}}_X f(x) \leq 0$ or $\tilde{\mathcal{L}}_X f(x) = \emptyset$ for all $x \in f^{-1}(\leq f(x_0), x_0)$. Then $f^{-1}(\leq f(x_0), x_0)$ is strongly invariant for* (2.7)*. Let*

$$Z_{X,f} = \{x \in \mathbb{R}^N \mid 0 \in \tilde{\mathcal{L}}_X f(x)\}\,.$$

Then, any solution $x : [t_0, +\infty) \to \mathbb{R}^N$ of (2.7) *starting from x_0 converges to the*

largest weakly invariant set M contained in $\overline{Z}_{X,f} \cap f^{-1}(\leq f(x_0), x_0)$. Furthermore, if the set M is a finite collection of points, then the limit of all solutions starting at x_0 exists and equals one of them.

The proof of the last fact in the theorem statement is the same as in the smooth case, since it only relies on the continuity of the trajectory.

Chapter 3

Averaging Over Acyclic Digraphs

In the literature, many researchers have used averaging algorithms to solve consensus problems. The spirit of averaging algorithms is to let the state of each agent evolve according to the (weighted) average of the state of its neighbors. Averaging algorithms has been studied both in continuous time [7, 13, 14, 15] and in discrete time [16, 15, 17, 18, 19, 20, 21, 22]. In [7], averaging algorithms are investigated via graph Laplacians [23] under a variety of assumptions, including fixed and switching communication topologies, time delays, and directed and undirected information flow. In [13], a series of consensus protocols are presented, based on the regular averaging algorithms, to drive the agents to agree upon the value of the power mean. A theoretical explanation for the consensus behavior of the Vicsek model [24] is provided in [17], see also the early work in [16], while [15] extends the results of [17] to the case of directed topology for both continuous and discrete update schemes. The work [18] adopts a set-valued Lyapunov approach to analyze the convergence properties of averaging algorithms, which is generalized in [19] to the case

of time delays. Asynchronous averaging algorithms are studied in [20]. The work [21] analyzes the averaging algorithms in the framework of partial difference equations over graphs [25]. The works [8, 26] survey the results available for consensus problems using averaging algorithms.

The contributions of this chapter is the investigation of the properties of averaging algorithms over acyclic digraphs with fixed and controlled-switching topologies. Our first contribution is a novel matrix representation of the disagreement function associated with a directed graph. Secondly, we prove that averaging over an fixed acyclic graph drives the agents to an equilibrium determined by the so-called "sinks" of the graph. Finally, we show that averaging over controlled-switching acyclic digraphs also makes the agents converge to the set of equilibria under suitable state-dependent switching signals.

3.1 Disagreement functions

Given a digraph $\mathcal{G}$ of order n, the *disagreement function* $\Phi_{\mathcal{G}} : \mathbb{R}^n \to \mathbb{R}$ is defined by

$$\Phi_{\mathcal{G}}(x) = \frac{1}{2} \sum_{i,j=1}^{n} a_{ij}(x_j - x_i)^2. \tag{3.1}$$

To the best of the authors' knowledge, the following is a novel result.

Proposition 3.1.1 (Matrix representation of disagreement)**.** *Given a digraph $\mathcal{G}$ of order n, the disagreement function $\Phi_{\mathcal{G}} : \mathbb{R}^n \to \mathbb{R}$ is the quadratic form associated with the symmetric positive-semidefinite matrix*

$$P(\mathcal{G}) = \frac{1}{2}(D_{\text{out}}(\mathcal{G}) + D_{\text{in}}(\mathcal{G}) - \mathcal{A}(\mathcal{G}) - \mathcal{A}(\mathcal{G})^T).$$

Moreover, $P(\mathcal{G})$ is the graph Laplacian of the mirror graph $\hat{\mathcal{G}}$, that is, $P(\mathcal{G}) = L(\hat{\mathcal{G}}) = \frac{1}{2}\Big(L(\mathcal{G}) + L(\tilde{\mathcal{G}})\Big)$.

Proof. For $x \in \mathbb{R}^n$, we compute

$$\begin{aligned} x^T P(\mathcal{G}) x &= \frac{1}{2} x^T (D_{\text{out}} + D_{\text{in}} - \mathcal{A} - \mathcal{A}^T) x \\ &= \frac{1}{2}\Big(\sum_{i,j=1}^{n} a_{ij} x_i^2 + \sum_{i,j=1}^{n} a_{ij} x_j^2 - 2 \sum_{i,j=1}^{n} a_{ij} x_i x_j \Big) \\ &= \frac{1}{2}\Big(\sum_{i,j=1}^{n} a_{ij} (x_i^2 + x_j^2 - 2 x_i x_j) \Big) \\ &= \frac{1}{2} \sum_{i,j=1}^{n} a_{ij} (x_j - x_i)^2 = \Phi_{\mathcal{G}}(x). \end{aligned}$$

Clearly P is symmetric. Since $\Phi_{\mathcal{G}}(x) \geq 0$ for all $x \in \mathbb{R}^n$, we deduce $P(\mathcal{G})$ is positive semidefinite. Since

$$(D(\hat{\mathcal{G}}))_{ii} = \sum_{j=1}^{n} \hat{a}_{ij} = \sum_{j=1}^{n} \frac{1}{2}(a_{ij} + a_{ji}),$$

we have $D(\hat{\mathcal{G}}) = \frac{1}{2}(D_{\text{out}}(\mathcal{G}) + D_{\text{in}}(\mathcal{G}))$. Hence,

$$\begin{aligned} L(\hat{\mathcal{G}}) &= D(\hat{\mathcal{G}}) - \mathcal{A}(\hat{\mathcal{G}}) \\ &= \frac{1}{2}(D_{\text{out}}(\mathcal{G}) + D_{\text{in}}(\mathcal{G})) - \frac{1}{2}(\mathcal{A}(\mathcal{G}) + \mathcal{A}(\mathcal{G})^T) = P(\mathcal{G}). \end{aligned}$$

The last inequality follows from the definitions of reverse and mirror graphs.

□

Remark 3.1.2. *Note that in general, $P(\mathcal{G}) \neq L(\mathcal{G})$. However, if the digraph $\mathcal{G}$ is balanced, then $D_{\text{out}}(\mathcal{G}) = D_{\text{in}}(\mathcal{G})$, and therefore,*

$$\begin{aligned} \Phi_{\mathcal{G}}(x) &= \frac{1}{2} x^T (D_{\text{out}}(\mathcal{G}) + D_{\text{in}}(\mathcal{G})) x - \frac{1}{2} x^T (\mathcal{A}(\mathcal{G}) + \mathcal{A}(\mathcal{G})^T) x \\ &= x^T D_{\text{out}}(\mathcal{G}) x - x^T \mathcal{A} x = x^T L(\mathcal{G}) x. \end{aligned}$$

This is the result usually presented in the literature on undirected graphs. •

3.2 Averaging plus connectivity achieves consensus

To each node $i \in \mathcal{U}$ of a digraph $\mathcal{G}$, we associate a state $x_i \in \mathbb{R}$, that obeys a first-order dynamics of the form

$$\dot{x}_i = u_i, \quad i \in \{1, \ldots, n\}.$$

We say that the nodes of a network have reached a *consensus* if $x_i = x_j$ for all $i, j \in \{1, \ldots, n\}$. Our objective is to design control laws u that guarantee that consensus is achieved starting from any initial condition, while u_i depends only on the state of the node i and of its neighbors in $\mathcal{G}$, for $i \in \{1, \ldots, n\}$. In other words, the closed-loop system asymptotically achieves consensus if, for any $x_0 \in \mathbb{R}^n$, one has that $x(t) \to \{\alpha(1, \ldots, 1) \mid \alpha \in \mathbb{R}\}$ when $t \to +\infty$. If the value α is the average of the initial state of the n nodes, then we say the nodes have reached *average-consensus*.

We refer to the following linear control law, often used in the literature on consensus (e.g., see [17, 20, 8]), as the *averaging protocol*:

$$u_i = \sum_{j=1}^{n} a_{ij}(x_j - x_i). \tag{3.2}$$

With this control law, the closed-loop system is

$$\dot{x}(t) = -L(\mathcal{G})x(t). \tag{3.3}$$

Next, we consider a family of digraphs $\{\mathcal{G}_1, \ldots, \mathcal{G}_m\}$ with the same vertex set $\{1, \ldots, n\}$. A *switching signal* is a map $\sigma : \overline{\mathbb{R}}_+ \times \mathbb{R}^n \to \{1, \ldots, m\}$. Given these objects, we can define the following switched dynamical system

$$\begin{aligned} \dot{x}(t) &= -L(\mathcal{G}_k)x(t), \\ k &= \sigma(t, x(t)). \end{aligned} \tag{3.4}$$

Note that the notion of solution for this system might not be well-defined for arbitrary switching signals. The properties of the linear system (3.3) and the system (3.4) under time-dependent switching signals have been investigated in [7, 15, 18, 27]. Here, we review some of these properties in the following two statements.

Theorem 3.2.1 (Averaging over a digraph)**.** *Let $\mathcal{G}$ be a digraph. The following statements hold:*

(i) System (3.3) *asymptotically achieves consensus if and only if $\mathcal{G}$ has a globally reachable node;*

(ii) If $\mathcal{G}$ is strongly connected, then system (3.3) *asymptotically achieves average-consensus if and only if $\mathcal{G}$ is balanced.*

Statement (i) is proved in [27, Section 2]. Statement (ii) is proved in [7, Section VII].

Theorem 3.2.2 (Averaging over switching digraphs)**.** *Let $\{\mathcal{G}_1, \ldots, \mathcal{G}_m\}$ be a family of digraphs with the same vertex set $\{1, \ldots, n\}$, and let $\sigma : \overline{\mathbb{R}}_+ \to \{1, \ldots, m\}$ be a piecewise constant function. The following statements hold:*

(i) System (3.4) *asymptotically achieves consensus if there exist infinitely many consecutive uniformly bounded time intervals such that the union of the switching graphs across each interval has a globally reachable node;*

(ii) If each $\mathcal{G}_i$, $i \in \{1, \ldots, m\}$, is strongly connected and balanced, then for any arbitrary piecewise constant function σ, the system (3.4) *globally asymptotically solves the* average-*consensus problem.*

Statement (i) is proved in [15, Section III B]. Statement (ii) is proved in [7, Section IX].

3.3 Averaging protocol over a fixed acyclic digraph

Here we characterize the convergence properties of the averaging protocol in equation (3.3) under different connectivity properties than the ones stated in Theorem 3.2.1, namely assuming that the given digraph is acyclic.

We start by reviewing some basic properties of acyclic digraphs. Given an acyclic digraph $\mathcal{G}$, every vertex of in-degree 0 is named *source*, and every vertex of out-degree 0 is named *sink*. Every acyclic digraph has at least one source and at least one sink. (Recall that sources and sinks can be identified by following any directed path on the digraph.) Given an acyclic digraph $\mathcal{G}$, we associate a nonnegative number to each vertex, called *depth*, in the following way. First, we define the depth of the sinks of $\mathcal{G}$ to be 0. Next, we consider the acyclic digraph that results from erasing the 0-depth vertices from $\mathcal{G}$ and the in-edges towards them; the depth of the sinks of this new acyclic digraph are defined to be 1. The higher depth vertices are defined recursively. This process is well-posed as any acyclic digraph has at least one sink. The depth of the digraph is the maximum depth of its vertices. For $n, d \in \mathbb{N}$, let $\mathcal{S}_{n,d}$ be the set of acyclic digraphs with vertex set $\{1, \dots, n\}$ and depth d.

Next, it is convenient to relabel the n vertices of the acyclic digraph $\mathcal{G}$ with depth d in the following way: (1) label the sinks from 1 to n_0, where n_0 is the number of sinks; (2) label the vertices of depth k from $\sum_{j=0}^{k-1} n_j + 1$ to $\sum_{j=0}^{k-1} n_j +$

n_k, where n_k is the number of vertices of depth k, for $k \in \{1, \dots, d\}$. Note that vertices with the same depth may be labeled in arbitrary order. With this labeling, the adjacency matrix $\mathcal{A}(\mathcal{G})$ is lower-diagonal with vanishing diagonal entries, and the Laplacian $L(\mathcal{G})$ takes the form

$$L(\mathcal{G}) = \begin{bmatrix} 0 & 0 & \dots & 0 \\ -a_{21} & \sum_{j=1}^{1} a_{2j} & \dots & 0 \\ \dots & \dots & \dots & \dots \\ -a_{n1} & -a_{n2} & \dots & \sum_{j=1}^{n-1} a_{nj} \end{bmatrix},$$

or, alternatively,

$$L(\mathcal{G}) = \begin{bmatrix} 0_{n_0 \times n_0} & 0_{n_0 \times (n-n_0)} \\ L_{21} & L_{22} \end{bmatrix}, \tag{3.5}$$

where $0_{k \times h}$ is the $k \times h$ matrix with vanishing entries, $L_{21} \in \mathbb{R}^{(n-n_0) \times n_0}$ and $L_{22} \in \mathbb{R}^{n-n_0 \times n-n_0}$. Clearly, all eigenvalues of L are non-negative and the zero eigenvalues are simple, as their corresponding Jordan blocks are 1×1 matrices.

Proposition 3.3.1 (Averaging over an acyclic digraph)**.** *Let $\mathcal{G}$ be an acyclic digraph of order n with n_0 sinks, assume its vertices are labeled according to their depth, and consider the dynamical system $\dot{x}(t) = -L(\mathcal{G})x(t)$ defined in* (3.3)*. The following statements hold:*

(i) The equilibrium set of (3.3) *is the vector subspace*

$$\ker L(\mathcal{G}) = \{(x_{\mathrm{s}}, x_{\mathrm{e}}) \in \mathbb{R}^{n_0} \times \mathbb{R}^{n-n_0} \mid x_{\mathrm{e}} = -L_{22}^{-1} L_{21} x_{\mathrm{s}}\}.$$

(ii) Each trajectory $x : \overline{\mathbb{R}}_+ \to \mathbb{R}^n$ of (3.3) *exponentially converges to the equilib-*

rium x^* defined recursively by

$$x_i^* = \begin{cases} x_i(0), & i \in \{1, \dots, n_0\}, \\ \dfrac{\sum_{j=1}^{i-1} a_{ij} x_j^*}{\sum_{j=1}^{i-1} a_{ij}}, & i \in \{n_0 + 1, \dots, n\}. \end{cases}$$

(iii) If $\mathcal{G}$ has unit depth, then the disagreement function $\Phi_{\mathcal{G}}$ is monotonically decreasing along any trajectory of (3.3).

Proof. Statement (i) is obvious. Statement (ii) follows from the fact that $-L_{22}$ is Hurwitz and from the equilibrium equality

$$0 = \sum_{j=1}^{i-1} a_{ij}(x_j^* - x_i^*) = \sum_{j=1}^{i-1} a_{ij} x_j^* - \Big(\sum_{j=1}^{i-1} a_{ij} \Big) x_i^*.$$

Regarding statement (iii), when the depth of $\mathcal{G}$ is 1, the adjacency matrix and the out-degree matrix are equal to, respectively,

$$\begin{bmatrix} 0_{n_0 \times n_0} & 0_{n_0 \times (n-n_0)} \\ -L_{21} & 0_{(n-n_0)\times(n-n_0)} \end{bmatrix}, \begin{bmatrix} 0_{n_0 \times n_0} & 0_{n_0 \times (n-n_0)} \\ 0_{(n-n_0)\times n_0} & L_{22} \end{bmatrix},$$

where L_{21} and L_{22} are defined in (3.5). Therefore, we compute

$$L(\tilde{\mathcal{G}}) = \begin{bmatrix} \tilde{L}_{11} & L_{21}^T \\ 0_{(n-n_0)\times n_0} & 0_{(n-n_0)\times(n-n_0)} \end{bmatrix},$$

where $\tilde{L}_{11} \in \mathbb{R}^{n_0 \times n_0}$. According to Proposition 3.1.1, we have

$$P(\mathcal{G}) = \frac{1}{2}\Big(L(\mathcal{G}) + L(\tilde{\mathcal{G}}) \Big)$$

The evolution of $\Phi_{\mathcal{G}}$ along a trajectory of $x : \overline{\mathbb{R}}_+ \to \mathbb{R}^n$ of (3.3) is given by

$$\begin{aligned} \frac{d}{dt}\Big(\Phi_{\mathcal{G}}(x(t)) \Big) &= -x(t)^T (L(\mathcal{G})^T P(\mathcal{G}) + P(\mathcal{G}) L(\mathcal{G})) x(t) \\ &= -x(t)^T L(\mathcal{G})^T L(\mathcal{G}) x(t) - x(t)^T L(\mathcal{G})^T L(\tilde{\mathcal{G}}) x(t) \\ &= -x(t)^T L(\mathcal{G})^T L(\mathcal{G}) x(t) \leq 0, \end{aligned}$$

where in the last equality we have used the fact that $L(\mathcal{G})^T L(\tilde{\mathcal{G}}) = L(\tilde{\mathcal{G}})^T L(\mathcal{G}) = 0_{n\times n}$. Note that $\Phi_{\mathcal{G}}$ is strictly decreasing unless $x(t) \in \ker L(\mathcal{G})$, i.e., the trajectory reaches an equilibrium. □

Remarks 3.3.2. *(i) If the digraph has a single sink, then the convergence statement in part (ii) of Proposition 3.3.1 is equivalent to part (i) of Theorem 3.2.1.*

(ii) The block decomposition of $L(\tilde{\mathcal{G}})$ holds only for digraphs with depth 1. Indeed, statement (iii) is not true for digraphs with depth larger than 1. The digraph in Figure 3.1 is a counterexample. •

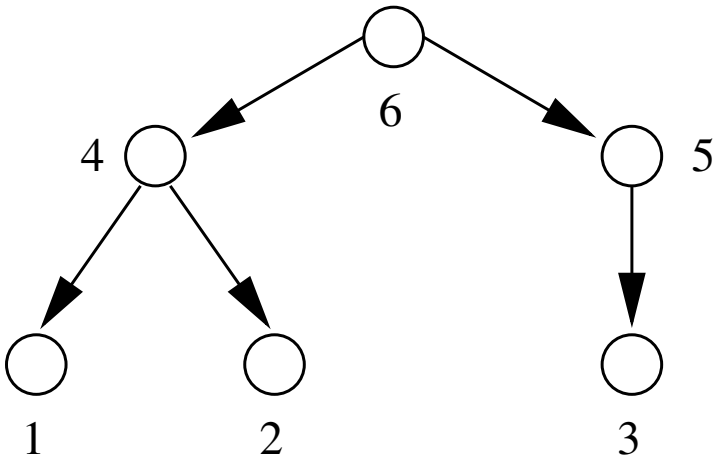

Figure 3.1: For this digraph of depth 2, the Lie derivative of the disagreement function (3.1) along the averaging flow (3.3) is indefinite.

3.4 Averaging protocol over switching acyclic digraphs

Given a family of digraphs $\Gamma = \{\mathcal{G}_1, \ldots, \mathcal{G}_m\}$ with vertex set $\{1, \ldots, n\}$, the *minimal disagreement function* $\Phi_\Gamma : \mathbb{R}^n \to \mathbb{R}$ is defined by

$$\Phi_\Gamma(x) = \min_{k \in \{1,\ldots,m\}} \Phi_{\mathcal{G}_k}(x). \tag{3.6}$$

Let $I(x) = \operatorname{argmin}\{\Phi_{\mathcal{G}_k}(x) \mid k \in \{1, \ldots, m\}\}$, we consider state-dependent switching signals $\sigma : \mathbb{R}^n \to \{1, \ldots, m\}$ with the property that $\sigma(x) \in I(x)$, that is, at each $x \in \mathbb{R}^n$, $\sigma(x)$ corresponds to the index of a graph with minimal disagreement. Clearly, for any such σ, one has $\Phi_\Gamma(x) = \Phi_{\mathcal{G}_{\sigma(x)}}(x)$. Before giving our result, we first point out a helpful fact.

Lemma 3.4.1. *Let $\Gamma = \{\mathcal{G}_1, \ldots, \mathcal{G}_m\} \subset \mathcal{S}_{n,1}$. If $\cup_{k \in \{1,\ldots,m\}} \mathcal{G}_k \in \mathcal{S}_{n,1}$, then for any $i, j \in \{1, \ldots, m\}$, we have*

$$L(\mathcal{G}_i)^T L(\tilde{\mathcal{G}}_j) = 0_{n \times n}.$$

Proof. Let $\mathcal{G} = \cup_{k \in \{1,\ldots,m\}} \mathcal{G}_k$. Since $\mathcal{G} \in \mathcal{S}_{n,1}$, so we have, by proper ordering of the nodes,

$$L(\mathcal{G}) = \begin{bmatrix} 0_{n_0 \times n_0} & 0_{n_0 \times (n-n_0)} \\ L_{21} & L_{22} \end{bmatrix}, \; L(\tilde{\mathcal{G}}) = \begin{bmatrix} \tilde{L}_{11} & L_{21}^T \\ 0_{(n-n_0)\times n_0} & 0_{(n-n_0)\times(n-n_0)} \end{bmatrix}.$$

For any $i \in \{1, \ldots, m\}$, $\mathcal{G}_i$ is a subgraph of $\mathcal{G}$, so that $L(\mathcal{G}_i)$ and $L(\tilde{\mathcal{G}}_i)$ share the same block decompositions as stated in the last equation. Hence, the statement follows immediately. □

Proposition 3.4.2 (Averaging over acyclic digraphs)**.** *Let $\Gamma = \{\mathcal{G}_1, \ldots, \mathcal{G}_m\} \subset \mathcal{S}_{n,1}$, and assume that $\cup_{k \in \{1,\ldots,m\}} \mathcal{G}_k \in \mathcal{S}_{n,1}$ and that $\sigma : \mathbb{R}^n \to \{1, \ldots, m\}$ satisfies*

$\sigma(x) \in I(x)$. *Consider the discontinuous dynamical system*

$$\dot{x}(t) = Y(x(t)) = -L(\mathcal{G}_k)x(t), \quad \textit{for} \quad k = \sigma(x(t)), \tag{3.7}$$

whose solutions are understood in the Filippov sense. The following statements hold:

(i) The point $x^* \in \mathbb{R}^n$ is an equilibrium for (3.7) *if and only if for each $i \in I(x^*)$, there exists scalars $\lambda_i \geq 0$ and $\sum_{i \in I(x^*)} \lambda_i = 1$, such that*

$$x^* \in \ker \Big(\sum_{i \in I(x^*)} \lambda_i L(\mathcal{G}_i) \Big). \tag{3.8}$$

In particular, if $I(x^*)$ contains only one element $k^* \in \{1, \ldots, m\}$, then (3.8) *can be simplified to*

$$x^* \in \ker L(\mathcal{G}_{k^*}). \tag{3.9}$$

(ii) Each trajectory $x : \overline{\mathbb{R}}_+ \to \mathbb{R}^n$ of (3.7) *converges to the set of equilibria.*

(iii) The minimum disagreement function Φ_Γ is monotonically non-increasing along any trajectory $x : \overline{\mathbb{R}}_+ \to \mathbb{R}^n$ of (3.7).

Proof. We investigate first smoothness of Φ_Γ. Because $-\Phi_\Gamma$ is the maximum of the smooth functions $-\Phi_{\mathcal{G}_k}$, by Proposition 2.4.4, we know that Φ_Γ is locally Lipschitz and has generalized gradient

$$\partial \Phi_\Gamma(x) = \operatorname{co}\{2P(\mathcal{G}_i)x \mid i \in I(x)\}.$$

Let $a \in \tilde{\mathcal{L}}_Y \Phi_\Gamma(x)$, then by definition, there exists $\omega = -\sum_{i \in I(x)} \lambda_i L(\mathcal{G}_i)x$, where, for each $i \in I(x)$, $\lambda_i \geq 0$ and $\sum_{i \in I(x)} \lambda_i = 1$, such that $a = \omega^T \zeta$ for all $\zeta \in$

$\partial\Phi_\Gamma(x)$. In particular, for $\zeta = \sum_{i\in I(x)} 2\lambda_i P(\mathcal{G}_i)x \in \partial\Phi_\Gamma(x)$, we have

$$\begin{aligned}
a &= \Big(-\sum_{i\in I(x)} \lambda_i L(\mathcal{G}_i)x\Big)^T \Big(\sum_{i\in I(x)} 2\lambda_i P(\mathcal{G}_i)x\Big) \\
&= -x^T\Big(\sum_{i\in I(x)} \lambda_i L(\mathcal{G}_i)\Big)^T \Big(\sum_{i\in I(x)} \lambda_i (L(\mathcal{G}_i) + L(\tilde{\mathcal{G}}_i))\Big)x \\
&= -x^T\Big(\sum_{i\in I(x)} \lambda_i L(\mathcal{G}_i)\Big)^T \Big(\sum_{i\in I(x)} \lambda_i L(\mathcal{G}_i)\Big)x - x^T\Big(\sum_{i\in I(x)} \lambda_i L(\mathcal{G}_i)^T\Big)\Big(\sum_{i\in I(x)} \lambda_i L(\tilde{\mathcal{G}}_i)\Big)x \\
&= -x^T\Big(\sum_{i\in I(x)} \lambda_i L(\mathcal{G}_i)\Big)^T \Big(\sum_{i\in I(x)} \lambda_i L(\mathcal{G}_i)\Big)x \leq 0,
\end{aligned}$$

where in the last equality we have used Lemma 3.4.1. Moreover,

$$a = 0 \quad \Longleftrightarrow \quad x \in \ker\Big(\sum_{i\in I(x)} \lambda_i L(\mathcal{G}_i)\Big).$$

In particular, if x is not at any switching surface, then $I(x)$ is a set with only one element $k \in \{1, \dots, m\}$ and $\partial\Phi_\Gamma(x) = 2P(\mathcal{G}_k)x$. Therefore, $\tilde{\mathcal{L}}_Y\Phi_\Gamma(x) = 0$ if and only if $x \in \ker L(\mathcal{G}_k)$. Therefore, we conclude that for $x \in \mathbb{R}^n$ and $a \in \tilde{\mathcal{L}}_Y\Phi_\Gamma(x)$, we have $a \leq 0$, i.e., $\max \tilde{\mathcal{L}}_Y\Phi_\Gamma(x) \leq 0$ and statement (i) is true. Resorting to the LaSalle Invariance Principle (Theorem 2.5.2), we deduce that any trajectory $x : \overline{\mathbb{R}}_+ \to \mathbb{R}^n$ of (3.7) converges to the set of equilibria as stated in statement (i) and statement (iii) is clear. □

Remarks 3.4.3. • *Statement (ii) in this theorem is weaker than statement (ii) in previous one in three ways: first, we are not able to characterize the limit point as a function of the initial state. Second, we require the depth 1 assumption, which is sufficient to ensure convergence, but possibly not necessary. Third, we establish only convergence to a set, rather than an individual point. It remains an open question to obtain necessary and sufficient conditions for convergence to a point.*

- *Although the statement (ii) is obtained only for digraphs of unit depth, this class of graphs is of interest in the forthcoming sections.*
-

Chapter 4

Discrete Coverage Control

In this chapter, we first review the multi-center optimization problem and the corresponding coverage control algorithm proposed in [1]. We then study the multi-center optimization problem in discrete space and derive a discrete coverage control law. This leads to a geometric object called the discrete Voronoi graph. Finally, we show that the discrete coverage control law is an averaging algorithm over a certain set of acyclic digraphs. Discrete locational optimization problems are discussed in [2, 28, 29].

We will consider motion coordination problems for a group of robots described by first order integrators. In other words, we assume that n robotic agents are placed at locations $p_1, \ldots, p_n \in \mathbb{R}^2$ and that they move according to

$$\dot{p}_i = u_i, \quad i \in \{1, \ldots, n\}. \tag{4.1}$$

We denote by P the vector of positions $(p_1, \ldots, p_n) \in (\mathbb{R}^2)^n$. Additionally, we define

$$\mathcal{S}_{\text{coinc}} = \{(p_1, \ldots, p_n) \in (\mathbb{R}^2)^n \mid p_i = p_j \text{ for some } i \neq j\},$$

and, for $P \notin \mathcal{S}_{\text{coinc}}$, we let $\{V_i(P)\}_{i\in\{1,\dots,n\}}$ denote the Voronoi partition generated by P, we illustrate this notion in Figure 4.1 and refer to [2] for a comprehensive treatment on Voronoi partitions.

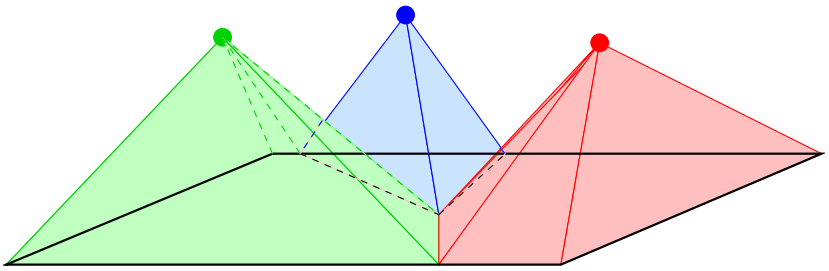

Figure 4.1: The Voronoi partition of a rectangle in the plane. We depict the generators $p_1, \dots, p_n$ elevated from the plane for intuition's sake.

4.1 Continuous and discrete multi-center functions

In this section we present a class of locational optimization problems in both continuous and discrete settings. It would be possible to provide a unified treatment using generalized functions and distributions, but we avoid it here for concreteness' sake.

Let Q be a convex polygon in $\mathbb{R}^2$ including its interior and let $\phi : \mathbb{R}^2 \to \overline{\mathbb{R}}_+$ be a bounded and measurable function whose support is Q. Analogously, let $\{q_1, \dots, q_N\} \subset \mathbb{R}^2$ be a pointset and $\{\phi_1, \dots, \phi_N\}$ be nonnegative weights associated to them. Given a non-increasing function $f : \overline{\mathbb{R}}_+ \to \mathbb{R}$, we consider the *continuous* and *discrete multi-center functions* $\mathcal{H} : (\mathbb{R}^2)^n \to \mathbb{R}$ and $\mathcal{H}_{\text{dscrt}}$:

$(\mathbb{R}^2)^n \to \mathbb{R}$ defined by

$$\mathcal{H}(P) = \int_Q \max_{i\in\{1,\dots,n\}} f(\|q-p_i\|)\phi(q)dq,$$
$$\mathcal{H}_{\text{dscrt}}(P) = \sum_{j=1}^{N} \max_{i\in\{1,\dots,n\}} \phi_j f(\|q_j-p_i\|).$$

Now we define

$$\mathcal{S}_{\text{equid}} = \{(p_1,\dots,p_n)\in(\mathbb{R}^2)^n \mid \|q-p_i\| = \|q-p_k\| = d(q) \\ \text{for some } q\in\{q_1,\dots,q_N\} \text{ and for some } i\neq k\},$$

where $d(q) = \min_{j\in\{1,\dots,n\}}\|q-p_j\|$. In other words, if $P\notin\mathcal{S}_{\text{equid}}$, then no point q_j is equidistant to two or more nearest robots. Note that $\mathcal{S}_{\text{equid}}$ is a set of measure zero because it is the union of the solutions of a finite number of algebraic equations. Using Voronoi partitions, for $P\notin\mathcal{S}_{\text{coinc}}$, we may write

$$\mathcal{H}(P) = \sum_{i=1}^{n}\int_{V_i(P)} f(\|q-p_i\|)\phi(q)dq,$$
$$\mathcal{H}_{\text{dscrt}}(P) = \sum_{i=1}^{n}\sum_{q_j\in V_i(P)} \frac{\phi_j}{\text{card}(q_j,P)} f(\|q_j-p_i\|)$$
$$= \sum_{i=1}^{n}\left(\sum_{q_j\in \overset{\circ}{V}_i(P)} \phi_j f(\|q_j-p_i\|) + \sum_{q_j\in\partial V_i(P)} \frac{\phi_j}{\text{card}(q_j,P)} f(\|q_j-p_i\|)\right),$$

where $\text{card}:\mathbb{R}^2\times(\mathbb{R}^2)^n\to\{1,\dots,n\}$ denotes the number of indices k for which $\|q_j-p_k\| = \min_{i\in\{1,\dots,n\}}\|q_j-p_i\|$. It is easy to see that card is distributed over the Voronoi graph and if q_j is a point in the interior of $V_i(P)$, then $\text{card}(q_j,P)=1$. For $P\notin\mathcal{S}_{\text{coinc}}\cup\mathcal{S}_{\text{equid}}$, we have

$$\mathcal{H}_{\text{dscrt}}(P) = \sum_{i=1}^{n}\sum_{q_j\in\overset{\circ}{V}_i(P)} \phi_j f(\|q_j-p_i\|).$$

Remark 4.1.1. *The function f plays the role of a performance function. If $\{p_1,\dots,p_n\}$ are the locations of n sensors, and if events take place inside the environment Q with*

likelihood ϕ, then $f(\|q - p_i\|)$ is the quality of service provided by sensor i. It will therefore be of interest to find local maxima for $\mathcal{H}$ and $\mathcal{H}_{\text{dscrt}}$. These types of optimal sensor placement spatial resource allocation problems are the subject of a discipline called locational optimization [2, 28, 1]. •

The following result is discussed in[30] for the continuous multi-center function.

Proposition 4.1.2 (Partial derivatives of $\mathcal{H}$)**.** *If f is locally Lipschitz, then $\mathcal{H}$ is locally Lipschitz on Q^n. Further, if f is differentiable, then $\mathcal{H}$ is differentiable on $Q^n \setminus \mathcal{S}_{\text{coinc}}$, and, for each $i \in \{1, \ldots, n\}$,*

$$\frac{\partial \mathcal{H}}{\partial p_i}(P) = \int_{V_i(P)} \frac{\partial}{\partial p_i} f(\|q - p_i\|)\phi(q)dq.$$

We obtain the corresponding properties of $\mathcal{H}_{\text{dscrt}}$ via nonsmooth analysis as the following proposition.

Proposition 4.1.3 (Generalized gradient of $\mathcal{H}_{\text{dscrt}}$)**.** *If f is locally Lipschitz, then $\mathcal{H}_{\text{dscrt}}$ is locally Lipschitz on Q^n. Further, if f is differentiable, then $\mathcal{H}_{\text{dscrt}}$ is regular on Q^n and its generalized gradient satisfies*

$$\partial \mathcal{H}_{\text{dscrt}}(P) = \sum_{j=1}^{N} \phi_j \operatorname{co} \left\{ \frac{\partial}{\partial P} f(\|q_j - p_k\|) \;\middle|\; k \in I(q_j, P) \right\},$$

where $I(q_j, P)$ is the set of indices k for which $f(\|q_j - p_k\|) = \max_{i \in \{1,\ldots,n\}} f(\|q_j - p_i\|)$, and in particular, if $P \notin \mathcal{S}_{\text{coinc}} \cup \mathcal{S}_{\text{equid}}$, then $\mathcal{H}_{\text{dscrt}}$ is differentiable at P, and for each $i \in \{1, \ldots, n\}$

$$\frac{\partial}{\partial p_i} \mathcal{H}_{\text{dscrt}}(P) = \sum_{q_j \in \overset{\circ}{V}_i(P)} \phi_j \frac{\partial}{\partial p_i} f(\|q_j - p_i\|).$$

Proof. We re-write here $\mathcal{H}_{\text{dscrt}}$ as

$$\mathcal{H}_{\text{dscrt}}(P) = \sum_{j=1}^{N} \max_{i\in\{1,\dots,n\}} \phi_j f(\|q_j - p_i\|) = \sum_{j=1}^{N} \phi_j F_j(P),$$

where, for each $j \in \{1, \dots, N\}$,

$$F_j(P) = \max_{i\in\{1,\dots,n\}} f(\|q_j - p_i\|).$$

We first investigate the smoothness of $F_j(P)$. By Proposition 2.4.4, it is easy to see that if f is locally Lipschitz, then $F_j(P)$ is locally Lipschitz on Q^n, so is $\mathcal{H}_{\text{dscrt}}(P)$.

Additionally, if f is differentiable, then $F_j(P)$ is regular on Q^n, with generalized derivative

$$\partial F_j(P) = \operatorname{co}\left\{ \frac{\partial}{\partial P} f(\|q_j - p_i\|) \;\middle|\; i \in I(q_j, P) \right\},$$

where $I(q_j, P)$ is the set of indexes k for which $f(\|q_j - p_k\|) = F_j(P)$. Since $\mathcal{H}_{\text{dscrt}}(P)$ is a finite sum of $F_j(P)$ with nonnegative weights ϕ_j, so $\mathcal{H}_{\text{dscrt}}(P)$ is also regular (cf. Proposition 2.4.2) on Q^n, with the regularity of $F_j(P)$, we obtain further the generalized gradient of $\mathcal{H}_{\text{dscrt}}(P)$ as

$$\partial \mathcal{H}_{\text{dscrt}}(P) = \sum_{j=1}^{N} \phi_j \operatorname{co}\left\{ \frac{\partial}{\partial P} f(\|q_j - p_k\|) \;\middle|\; k \in I(q_j, P) \right\}.$$

The expression for the partial derivative away from $\mathcal{S}_{\text{coinc}} \cup \mathcal{S}_{\text{equid}}$ is easy to see. □

Let $\partial_i \mathcal{H}_{\text{dscrt}}(P)$ denote the i^{th} block component of $\partial \mathcal{H}_{\text{dscrt}}(P)$, the following result is a consequence of Proposition 4.1.3.

Corollary 4.1.4. *If f is differentiable, then for each $i \in \{1, \dots, n\}$,*

$$\partial_i \mathcal{H}_{\text{dscrt}}(P) \subset \sum_{q_j \in \overset{\circ}{V}_i(P)} \phi_j \frac{\partial}{\partial p_i} f(\|q_j - p_i\|) + \sum_{q_j \in \partial V_i(P)} \phi_j \operatorname{co}\left\{ \begin{bmatrix} 0 \\ 0 \end{bmatrix}, \frac{\partial}{\partial p_i} f(\|q_j - p_i\|) \right\}.$$

For particular choices of f, the multi-center functions and their partial derivatives may simplify. For example, if $f(x) = -x^2$, the partial derivative of the multi-center function $\mathcal{H}$ reads (for $P \notin \mathcal{S}_{\text{coinc}}$)

$$\frac{\partial \mathcal{H}}{\partial p_i}(P) = 2M_{V_i(P)}(C_{V_i(P)} - p_i),$$

where mass and the centroid of $W \subset Q$ are

$$M_W = \int_W \phi(q)\, dq, \quad C_W = \frac{1}{M_W} \int_W q\, \phi(q)\, dq.$$

Additionally, the critical points P^* of $\mathcal{H}$ have the property that $p_i^* = C_{V_i(P^*)}$, for $i \in \{1, \dots, n\}$; these are called *centroidal Voronoi configurations*. Analogously, if $f(x) = -x^2$, the discrete multi-center function $\mathcal{H}_{\text{dscrt}}$ reads

$$\mathcal{H}_{\text{dscrt}}(P) = -\sum_{j=1}^{N} \max_{i \in \{1, \dots, n\}} \phi_j \|q_j - p_i\|^2,$$

and its generalized gradient is

$$\partial \mathcal{H}_{\text{dscrt}}(P) = \sum_{j=1}^{N} \phi_j \operatorname{co}\left\{ 2(q_j - p_k) \frac{\partial p_k}{\partial P} \;\middle|\; k \in I(q_j, P) \right\}. \tag{4.2}$$

For each $j \in \{1, \dots, N\}$, assume the scalars λ_{ij}, $i \in I(q_j, P)$, satisfy

$$\lambda_{ij} \geq 0, \qquad \sum_{i \in I(q_j, P)} \lambda_{ij} = 1. \tag{4.3}$$

Next, define $(M_{\text{dscrt}})_{V_i(P)}$ and $(C_{\text{dscrt}})_{V_i(P)}$, respectively, as

$$(M_{\text{dscrt}})_{V_i(P)} = \sum_{q_j \in \overset{\circ}{V}_i(P)} \phi_j + \sum_{q_j \in \partial V_i(P)} \lambda_{ij} \phi_j = \sum_{q_j \in V_i(P)} \lambda_{ij} \phi_j,$$

$$(C_{\text{dscrt}})_{V_i(P)} = \begin{cases} p_i, & \text{if } (M_{\text{dscrt}})_{V_i(P)} = 0, \\ \dfrac{1}{(M_{\text{dscrt}})_{V_i(P)}} \left(\displaystyle\sum_{q_j \in V_i(P)} \lambda_{ij} \phi_j q_j \right), & \text{otherwise.} \end{cases}$$

Lemma 4.1.5. *Given $f(x) = -x^2$, P^* is a critical point of $\partial H_{\text{dscrt}}$, i.e., $0 \in \partial H_{\text{dscrt}}(P^*)$, if and only if for any $j \in \{1, \dots, N\}$, there exist λ_{ij} as in* (4.3)*, such that $p_i^* = (C_{\text{dscrt}})_{V_i(P^*)}$, for each $i \in \{1, \dots, n\}$.*

Proof. Given scalar satisfying (4.3), define

$$w = \sum_{j=1}^{N} \phi_j \sum_{k \in I(q_j, P)} 2\lambda_{kj}(q_j - p_k^*) \frac{\partial p_k}{\partial P},$$

then it is clear that $w \in \partial \mathcal{H}_{\text{dscrt}}(P^*)$. Let w_i denotes the i^{th} component of w, since

$$w_i = 2 \sum_{q_j \in V_i(P^*)} \lambda_{ij} \phi_j (q_j - p_i^*) = 2 \sum_{q_j \in V_i(P^*)} \lambda_{ij} \phi_j (q_j - (C_{\text{dscrt}})_{V_i(P^*)}) = 0,$$

so $w = 0$ and $0 \in \partial H_{\text{dscrt}}(P^*)$.

On the other hand, if P^* is a critical point, then there exists scalars λ_{ij} satisfying (4.3), such that

$$w = \sum_{j=1}^{N} \phi_j \sum_{k \in I(q_j, P)} 2\lambda_{kj}(q_j - p_k^*) \frac{\partial p_k}{\partial P} = 0,$$

which implies, for each $i \in \{1, \dots, n\}$

$$w_i = 2 \sum_{q_j \in V_i(P^*)} \lambda_{ij} \phi_j (q_j - p_i^*) = 0,$$

Solve this linear equation, we obtain

$$p_i^* = (C_{\text{dscrt}})_{V_i(P^*)}, \qquad i \in \{1, \dots, n\}.$$

□

4.2 Continuous and discrete coverage control

Based on the expressions obtained in the previous subsection, it is possible to design motion coordination algorithms for the robots $p_1, \ldots, p_n$. We call *continuous* and *discrete coverage control* the problem maximizing the multicenter functions $\mathcal{H}$ and $\mathcal{H}_{\text{dscrt}}$, respectively. The continuous problem is studied in [1]. We simply impose that the locations $p_1, \ldots, p_n$ follow a gradient ascent law defined over the set $Q^n \setminus \mathcal{S}_{\text{coinc}}$. Formally, we set

$$u_i = k_{\text{prop}} \frac{\partial \mathcal{H}}{\partial p_i}(P), \tag{4.4}$$

where k_{prop} is a positive gain. Note that this law is distributed in the sense that each robot only needs information about its Voronoi cell in order to compute its control.

For discrete coverage control, we adopt the following discontinuous control law, for each robot $i \in \{1, \ldots, n\}$

$$u_i = k_{\text{prop}} X_i(P), \tag{4.5}$$

where $X_i : Q^n \to \mathbb{R}^2$ is defined as

$$X_i(P) = \sum_{q_j \in V_i(P)} \frac{\phi_j}{\mathtt{card}(q_j, P)} \frac{\partial}{\partial p_i} f(\|q_j - p_i\|).$$

Note that X_i is continuous at $P \in Q^n \setminus \mathcal{S}_{\text{coinc}} \cup \mathcal{S}_{\text{equid}}$, and satisfies

$$X_i(P) = \frac{\partial \mathcal{H}_{\text{dscrt}}}{\partial p_i}(P).$$

Like control law (4.4), the discontinuous control law (4.5) is also distributed. Define the vector field $X = [X_1, X_2, \ldots, X_n]^T$, we have

$$\dot{P} = k_{\text{prop}} X(P). \tag{4.6}$$

Since $X(P)$ is discontinuous at $P \in \mathcal{S}_{\text{coinc}} \cup \mathcal{S}_{\text{equid}}$, we understand the solution of this equation in the Filippov sense following [4], and the existence of Filippov solution is guaranteed. We then investigate the properties of the solution and analysis the convergence of (4.4) and (4.5).

Proposition 4.2.1 (Continuous coverage control; [1, 30])**.** *For the closed-loop systems induced by equation* (4.4) *starting at* $P_0 \in Q^n \setminus \mathcal{S}_{\text{coinc}}$*, the agents location converges asymptotically to the set of critical points of* $\mathcal{H}$*.*

Proposition 4.2.2 (Discrete coverage control)**.** *For the closed-loop systems induced by equation* (4.5) *starting at* $P_0 \in Q^n \setminus \mathcal{S}_{\text{coinc}}$*, the agents location converges asymptotically to the set of critical points of* $\mathcal{H}_{\text{dscrt}}$*.*

Proof. Note that

$$K[k_{\text{prop}}\, X](P) = k_{\text{prop}} \partial \mathcal{H}_{\text{dscrt}}(P).$$

Given this property, the following proof is essentially the same as the proof of Proposition 2.9 in [31]. We refer the interested reader to [31] for technical details. □

4.3 Discretizing continuous settings

In this section we discuss the relationship between the discretization of continuous locational optimization problems and discrete locational optimization problems.

As before, let Q be a convex polygon in $\mathbb{R}^2$ including its interior, and let $\phi : \mathbb{R}^2 \to \overline{\mathbb{R}}_+$ be a bounded and measurable function whose support is Q. We shall

consider a sequence of pointsets $\{q_1^k, \ldots, q_{N_k}^k\}_{k\in\mathbb{N}} \subset \mathbb{R}^2$ and of nonnegative weights $\{\phi_1^k, \ldots, \phi_{N_k}^k\}_{k\in\mathbb{N}}$. Accordingly, we can define a sequence of discrete multi-center functions $\mathcal{H}_{\text{dscrt}}^k$, for $k \in \mathbb{N}$. The sequence $\{q_1^k, \ldots, q_{N_k}^k\}_{k\in\mathbb{N}} \subset \mathbb{R}^2$ is *dense*[1] in Q if, for all $q \in Q$,

$$\lim_{k\to+\infty} \min\{\|q - z\| \mid z \in \{q_1^k, \ldots, q_{N_k}^k\}\} = 0.$$

Given a pointset $q_1, \ldots, q_N$, let $V(q_1, \ldots, q_N)$ denote the Voronoi partition it generates and define the associated weights

$$\phi_j = \int_{V_j(q_1,\ldots,q_N)} \phi(q)dq. \tag{4.7}$$

Proposition 4.3.1 (Consistent discretization)**.** *Assume that f is continuous almost everywhere, that the sequence $\{q_1^k, \ldots, q_{N_k}^k\}_{k\in\mathbb{N}} \subset \mathbb{R}^2$ is dense in Q, and that the sequence of weights are defined according to* (4.7)*. Then $\{\mathcal{H}_{\text{dscrt}}^k\}_{k\in\mathbb{N}}$ converges pointwise to $\mathcal{H}$, that is, for all $P \in Q^n$,*

$$\lim_{k\to+\infty} \mathcal{H}_{\text{dscrt}}^k(P) = \mathcal{H}(P).$$

Additionally, if f is continuously differentiable, then for $P \in Q^n \setminus \mathcal{S}_{\text{coinc}}$ and each $i \in \{1, \ldots, n\}$, any sequence $x_k \in \partial_i \mathcal{H}_{\text{dscrt}}^k(P)$, $k \in \mathbb{N}$, satisfies

$$\lim_{k\to+\infty} x_k = \frac{\partial \mathcal{H}}{\partial p_i}(P).$$

Proof. For $k \in \mathbb{N}$, given the pointset $\{q_1^k, \ldots, q_{N_k}^k\}$, we define the projection $\text{proj}_k : Q \to \{q_1^k, \ldots, q_{N_k}^k\}$ by

$$\text{proj}_k(q) = \text{argmin}\{\|q - z\| \mid z \in \{q_1^k, \ldots, q_{N_k}^k\}\}.$$

[1]This is equivalent to asking that the sequence has *vanishing dispersion*; the dispersion of a pointset $\{q_1, \ldots, q_N\}$ in the compact set Q is $\max_{q\in Q} \min_{z\in\{q_1,\ldots,q_N\}} \|q - z\|$.

Because of the vanishing dispersion property, we know that, for all $q \in Q$,

$$\lim_{k \to +\infty} \operatorname{proj}_k(q) = q. \tag{4.8}$$

Therefore, we compute

$$\begin{aligned}
\mathcal{H}^k_{\text{dscrt}}(P) &= \sum_{j=1}^{N_k} \max_{i \in \{1,\dots,n\}} f(\|q_j^k - p_i\|) \int_{V_j(q_1^k,\dots,q_{N_k}^k)} \phi(q) dq \\
&= \sum_{j=1}^{N_k} \int_{V_j(q_1^k,\dots,q_{N_k}^k)} \max_{i \in \{1,\dots,n\}} f(\|q_j^k - p_i\|) \phi(q) dq \\
&= \int_Q \max_{i \in \{1,\dots,n\}} f(\|\operatorname{proj}_k(q) - p_i\|) \phi(q) dq.
\end{aligned}$$

Because f is continuous almost everywhere, we have

$$\begin{aligned}
&\lim_{k \to +\infty} \mathcal{H}^k_{\text{dscrt}}(P) \\
&\quad = \lim_{k \to +\infty} \int_Q \max_{i \in \{1,\dots,n\}} f(\|\operatorname{proj}_{N_k}(q) - p_i\|) \phi(q) dq \\
&\quad = \int_Q \max_{i \in \{1,\dots,n\}} f(\|\lim_{k \to +\infty} \operatorname{proj}_{N_k}(q) - p_i\|) \phi(q) dq \\
&\quad = \int_Q \max_{i \in \{1,\dots,n\}} f(\|q - p_i\|) \phi(q) dq = \mathcal{H}(P).
\end{aligned}$$

Define

$$\partial_i^* \mathcal{H}^k_{\text{dscrt}}(P) = \sum_{q_j^k \in \overset{\circ}{V}_i(P)} \phi_j \frac{\partial}{\partial p_i} f(\|q_j^k - p_i\|) + \sum_{q_j^k \in \partial V_i(P)} \phi_j \operatorname{co}\left\{ \begin{bmatrix} 0 \\ 0 \end{bmatrix}, \frac{\partial}{\partial p_i} f(\|q_j^k - p_i\|) \right\}.$$

By Corollary 4.1.4, if f is differentiable, then $\partial_i \mathcal{H}^k_{\text{dscrt}}(P) \subset \partial_i^* \mathcal{H}^k_{\text{dscrt}}(P)$. Suppose $x_k^* \in \partial_i^* \mathcal{H}^k_{\text{dscrt}}(P)$, then there exists scalars $\lambda_{ij} \in [0, 1]$, such that

$$x_k^* = \sum_{q_j^k \in \overset{\circ}{V}_i(P)} \phi_j \frac{\partial}{\partial p_i} f(\|q_j^k - p_i\|) + \sum_{q_j^k \in \partial V_i(P)} \lambda_{ij} \phi_j \frac{\partial}{\partial p_i} f(\|q_j^k - p_i\|). \tag{4.9}$$

Substitute (4.7) into (4.9), we obtain

$$x_k^* = \sum_{q_j^k \in \overset{\circ}{V}_i(P)} \int_{V_j(q_1^k,\dots,q_N^k)} \phi(q) \frac{\partial}{\partial p_i} f(\|q_j^k - p_i\|) dq + \sum_{q_j^k \in \partial V_i(P)} \int_{V_j(q_1^k,\dots,q_N^k)} \lambda_{ij} \phi(q) \frac{\partial}{\partial p_i} f(\|q_j^k - p_i\|) dq.$$

Since f is continuously differentiable, so for $P \in Q^n \setminus \mathcal{S}_{\text{coinc}}$, we have

$$\lim_{k \to +\infty} x_k^* = \int_{\overset{\circ}{V}_i(P)} \phi(q) \frac{\partial}{\partial p_i} f(\|q - p_i\|) dq + \begin{bmatrix} 0 \\ 0 \end{bmatrix} = \frac{\partial \mathcal{H}}{\partial p_i}(P).$$

Hence,

$$\lim_{k \to +\infty} x_k = \frac{\partial \mathcal{H}}{\partial p_i}(P).$$

□

4.4 The relationship between discrete coverage and averaging over switching acyclic digraphs

As above, let Q be a convex polygon, let $\{p_1, \dots, p_n\} \subset Q$ be the position of n robots, let $\{q_1, \dots, q_N\} \subset Q$ be N fixed points in Q with corresponding nonnegative weights $\{\phi_1, \dots, \phi_N\}$, and let $I(q_j, P)$ be the set of indices k for which $\|q_j - p_k\| = \min_{i \in \{1,\dots,n\}} \|q_j - p_i\|$. We begin by defining a useful digraph and a useful set of digraphs.

A *discrete Voronoi graph* $\mathcal{G}_{\text{dscrt-Vor}}$ is a digraph with $(n+N)$ vertices $\{p_1, \dots, p_n, q_1, \dots, q_N\}$, with N directed edges

$$\{(p_i, q_j) | \text{ for each } j \in \{1, \dots, N\}, \text{ pick one and only one } i \in I(q_j, P)\},$$

and with corresponding edge weights ϕ_j, for all $j \in \{1, \ldots, N\}$. We illustrate this graph in Figure 4.2. With our definition, it is possible for one vertex

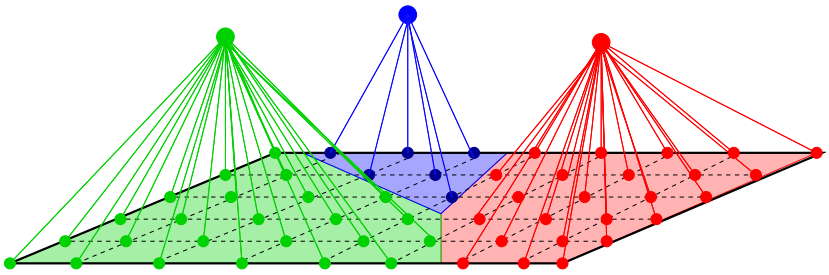

Figure 4.2: The discrete Voronoi graph over 3 robots and 6×9 grid points. This illustration is to be compared with the Voronoi partition illustrated in Figure 4.1. The edges have top/down direction.

set to generate multiple discrete Voronoi graphs. We will denote the nodes of $\mathcal{G}_{\text{dscrt-Vor}}$ by $Z = (z_1, \ldots, z_{n+N}) \in (\mathbb{R}^2)^{n+N}$, the weights by $a_{\alpha\beta}$, for $\alpha, \beta \in \{1, \ldots, n+N\}$, with the understanding that:

$$z_\alpha = \begin{cases} p_\alpha, & \text{if } \alpha \in \{1, \ldots, n\}, \\ q_{\alpha - n}, & \text{otherwise,} \end{cases}$$

and that the only non-vanishing weights are $a_{\alpha\beta} = \phi_j$ when $\beta = n + j$, for $j \in \{1, \ldots, N\}$, and when $\alpha \in \{1, \ldots, n\}$ corresponds to the robot p_α closest to q_j and (p_α, q_j) is a directed edge of the graph $\mathcal{G}_{\text{dscrt-Vor}}$. Note that $\mathcal{G}_{\text{dscrt-Vor}}$ depends upon Z. Since $\{q_1, \ldots, q_N\} \subset Q$ are fixed, when we need to emphasize this dependence, we will simply denote it as $\mathcal{G}_{\text{dscrt-Vor}}(P)$.

Let us now define a set of digraphs of which the discrete Voronoi graphs are examples. Let $F(N, n)$ be the set of functions from $\{1, \ldots, N\}$ to $\{1, \ldots, n\}$. Roughly speaking, a function in $F(N, n)$ assigns to each point q_j, $j \in \{1, \ldots, N\}$, a robot p_i, $i \in \{1, \ldots, n\}$. Given $h \in F(N, n)$, let $\mathcal{G}_h$ be the digraph with $(n+N)$

vertices $\{p_1, \ldots, p_n, q_1, \ldots, q_N\}$, with N directed edges

$$\{(p_{h(j)}, q_j)\}_{j\in\{1,\ldots,N\}},$$

and corresponding edge weights ϕ_j, $j \in \{1, \ldots, N\}$. With these notations, it holds that $\mathcal{G}_{\text{dscrt-Vor}}(P) = \mathcal{G}_{h^*(\cdot,P)}$ with any function $h^* : \{1, \ldots, N\} \times Q^n \to \{1, \ldots, n\}$ which satisfies

$$h^*(j, P) \in \operatorname{argmin}\{\|q_j - p_i\| \mid i \in \{1, \ldots, n\}\}.$$

Let us state a useful observation about these digraphs.

Lemma 4.4.1. *The set of digraphs $\mathcal{G}_h$, $h \in F(N, n)$, is a set of acyclic digraphs with unit depth, i.e., it is a subset of $\mathcal{S}_{n+N,1}$ (see definition in Subsection 3.3). Moreover, $\cup_{h\in F(N,n)} \mathcal{G}_h$ is an acyclic digraph with unit depth, i.e., $\cup_{h\in F(N,n)} \mathcal{G}_h \in \mathcal{S}_{n+N,1}$.*

For $h \in F(N, n)$, let us study appropriate disagreement functions for the digraph $\mathcal{G}_h$. We define the function $\Phi_{\mathcal{G}_h} : (\mathbb{R}^2)^{n+N} \to \mathbb{R}$ by

$$\begin{aligned}\Phi_{\mathcal{G}_h}(Z)|_{Z=(p_1,\ldots,p_n,q_1,\ldots,q_N)} &= \frac{1}{2}\sum_{\alpha,\beta=1}^{n+N} a_{\alpha\beta}\|z_\alpha - z_\beta\|^2 \\ &= \frac{1}{2}\sum_{j=1}^{N} \phi_j\|q_j - p_{h(j)}\|^2,\end{aligned}$$

because the weights $a_{\alpha\beta}$, $\alpha, \beta \in \{1, \ldots, n + N\}$ of the digraph $\mathcal{G}_h$ all vanish except for $a_{h(j),j} = \phi_j$, $j \in \{1, \ldots, N\}$.

We are now ready to state the main result of this section. The proof of the following theorem is based on simple book-keeping and is therefore omitted.

Theorem 4.4.2 (Discrete coverage control and averaging)**.** *The following statements hold:*

(i) The discrete multi-center function $\mathcal{H}_{\text{dscrt}}$ with $f(x) = -x^2$, and the minimum disagreement function over the set of digraphs $\mathcal{G}_h$, $h \in F(N,n)$, satisfy

$$\begin{aligned}
-\frac{1}{2}\mathcal{H}_{\text{dscrt}}(P) &= \frac{1}{2}\sum_{j=1}^{N} \min_{i\in\{1,\dots,n\}} \phi_j \|q_j - p_i\|^2 \\
&= \frac{1}{2}\sum_{j=1}^{N} \phi_j \|q_j - p_{h^*(j)}\|^2 \\
&= \Phi_{\mathcal{G}_{\text{dscrt-Vor}}}(p_1,\dots,p_n,q_1,\dots,q_N) \\
&= \min_{h\in F(N,n)} \Phi_{\mathcal{G}_h}(p_1,\dots,p_n,q_1,\dots,q_N).
\end{aligned}$$

(ii) For $P \notin \mathcal{S}_{\text{coinc}} \cup \mathcal{S}_{\text{equid}}$, the discrete coverage control law for $f(x) = -x^2$ and the averaging protocol over the discrete Voronoi digraph satisfy, for $i \in \{1,\dots,n\}$,

$$\frac{1}{2}\frac{\partial \mathcal{H}_{\text{dscrt}}}{\partial p_i}(P) = \sum_{q_j \in V_i(P)} \phi_j(q_j - p_i) = \sum_{\beta=1}^{n+N} a_{\alpha\beta}(z_\beta - z_\alpha),$$

where z_α and $a_{\alpha\beta}$, $\alpha,\beta \in \{1,\dots,n+N\}$, are nodes and weights of $\mathcal{G}_{\text{dscrt-Vor}}$. Accordingly, the discontinuous coverage control system (4.6), for $f(x) = -x^2$, and the averaging system (3.7) over the set of digraphs $\mathcal{G}_h$, $h \in F(N,n)$ satisfy, for $i \in \{1,\dots,n\}$,

$$\frac{1}{2}K[X_i](P) = K[Y_i](Z),$$

where $Z = (p_1,\dots,p_n,q_1,\dots,q_N)$, X_i and Y_i are the i^{th} 2-dimensional block component of X and Y, respectively.

(iii) Any $P^* \in Q^n$ is an equilibrium of the discrete coverage control system with $f(x) = -x^2$ if and only if $Z^* = (p_1^*,\dots,p_n^*,q_1,\dots,q_N)$ is an equilibrium of

system (3.7) *over the set of digraphs* $\mathcal{G}_h$, $h \in F(N,n)$, *that is:*

$$\forall j \in \{1,\dots,N\},\ \exists \lambda_{ij} \text{ as in (4.3), such that } p_i^* = (C_{\text{dscrt}})_{V_i(P^*)},\ \forall i \in \{1,\dots,n\},$$
$$\iff \quad \exists \mu_k \geq 0 \text{ and } \sum_k \mu_k = 1, \text{ such that } Z^* \in \ker\Big(\sum_k \mu_k L(\mathcal{G}^k_{\text{dscrt-Vor}}(Z^*))\Big),$$

where $\{\mathcal{G}^k_{\text{dscrt-Vor}}(Z^*)\}_k$ *are all possible discrete Voronoi graphs generated by* Z^*.

(iv) Given any initial position of robots $P_0 \in Q^n$, *the evolution of the discrete coverage control system* (4.6) *and the evolution of the averaging system* (3.7) *under the switching signal* $\sigma : Q^n \to \{\mathcal{G}_h \mid h \in F(N,n)\}$ *defined by* $\sigma(P) = \mathcal{G}_{\text{dscrt-Vor}}(Z)$ *are identical in the Filippov sense and, therefore, the two systems will converge to the same set of equilibrium placement of robots, as described in (iii).*

4.5 Numerical simulations

To illustrate the performance of the discrete coverage law as stated in Proposition 4.2.2 and to illustrate the accuracy of the discretization process, as analyzed in Proposition 4.3.1, we include some simulation results. The algorithms are implemented in `Matlab` as a single centralized program. As expected, the simulations for the discrete coverage law are computationally intensive with the increase in the resolution of the grid. We illustrate the performance of the closed-loop systems in Figures 4.3, 4.4, 4.5 and 4.6.

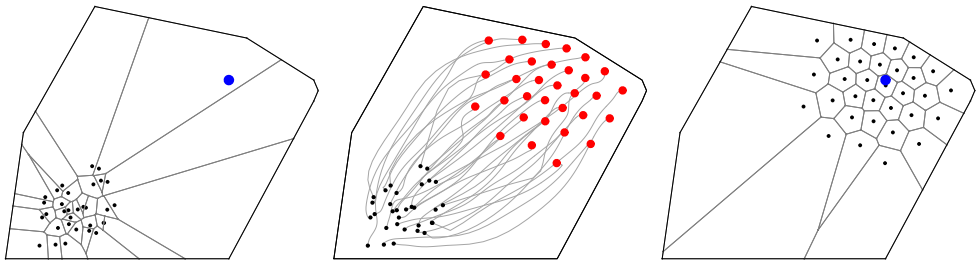

Figure 4.3: Continuous coverage law for 32 agents on a convex polygonal environment, with density function $\phi = \texttt{exp}(5.(-x^2 - y^2))$ centered about the gray point in the figure. The control gain in (4.4) is $k_{\text{prop}} = 1$ for all the vehicles. The left (respectively, right) figure illustrates the initial (respectively, final) locations and Voronoi partition. The central figure illustrates the gradient descent flow. Figure taken from [1].

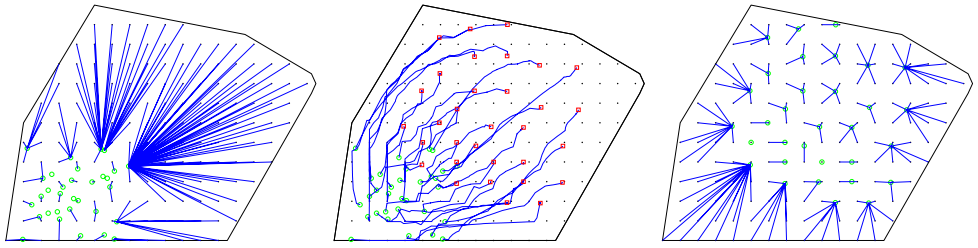

Figure 4.4: Simulation of discrete coverage law with 159 grid points.

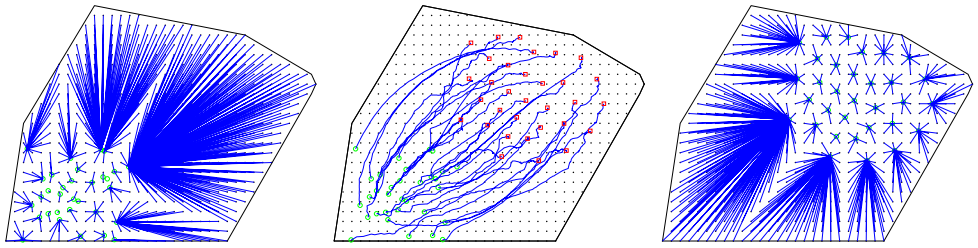

Figure 4.5: Simulation of discrete coverage law with 622 grid points.

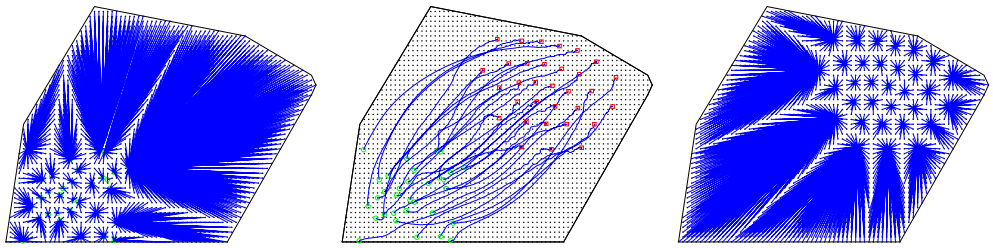

Figure 4.6: Simulation of discrete coverage law with 2465 grid points.

4.6 Generalization of ordinary coverage control

In previous sections of this chapter, we have discussed coverage control for a group of identical agents. All the agents are supposed to have the same sensing and communication capability. But in many practical applications, this is not always the case. We may have a group of agents with different sensing or communication capability. For instance, there is a group of UAVs in service, several of them are equipped with much more advanced sensors than others.

One possible solution of this kind of problems is to assign a weight ω_i to each agent i according to to its sensing or communication capability. This weight ω_i may be constant or changing corresponding some specific conditions. We define the *weighted* multi-center function in continuous space $\mathcal{H}_w : (\mathbb{R}^2)^n \to \mathbb{R}$ by

$$\mathcal{H}_w(P) = \int_Q \max_{i\in\{1,\dots,n\}} \frac{1}{\omega_i} f(\|q - p_i\|)\phi(q)dq,$$

which will generate a weighted Voronoi partition, as defined in Section 2.1.2, of the polygon Q. Then, we can investigate derivatives of $\mathcal{H}_w$ and design distributed control laws to optimize $\mathcal{H}_w$, as we did in Section 4.1 and Section 4.2. Similar generalization can be done to coverage control in discrete space. We

will develop these ideas in the future.

Chapter 5

Dynamic Consensus

Most consensus problems studied so far have been focusing on static inputs. However, in many practical applications, the nature of distributed control requires coordination among agents in a dynamic environment. Therefore, consensus on static inputs is not sufficient, and investigation on consensus on dynamic inputs is in need for many engineering situations. In section 5.1, we review the proportional dynamic average consensus estimator presented in [32]; and in section 5.2, we propose a dynamic maximum consensus estimator and verify its effectiveness by simulations.

5.1 Dynamic Average Consensus

For a group of n agents, suppose each agent $i \in \{1, \ldots, n\}$ maintains one time varying function $r_i(t)$, which is the measurement of some dynamic quantity of interest. The dynamic average consensus is the problem of tracking the

dynamic average of $r_i(t)$, for $i \in \{1, \ldots, n\}$. That is, we wish each agent to track the quantity

$$\bar{r}(t) = \frac{1}{n} \sum_{i=1}^{n} r_i(t).$$

Dynamic average consensus problems have recently been studied in [33, 32]. The authors of [32] proposed, based on the idea presented in [33], a proportional dynamic consensus estimator of following form, for each agent $i \in \{1, \ldots, n\}$,

$$\dot{w}_i(t) = -\gamma w_i(t) + \sum_{j \neq i} a_{ij}(t)[z_j(t) - z_i(t)], \tag{5.1}$$

$$z_i(t) = w_i(t) + r_i(t), \tag{5.2}$$

where $r_i(t) \in \mathbb{R}$ is the input, $z_i(t) \in \mathbb{R}$ is the decision output, $w_i(t)$ is the internal estimator state, γ is a global parameter, and $a_{ij}(t)$ are piecewise-continuous gains. Since each agent can only communicate with its neighbors, we have $a_{ij}(t) = 0$ when agent i can not sense agent j's decision output z_j at time t. Let $w(t) = [w_1(t), \ldots, w_n(t)]^T$, $z(t) = [z_1(t), \ldots, z_n(t)]^T$, $r(t) = [r_1(t), \ldots, r_n(t)]^T$, and $L(t)$ be the Laplacian of the communication graph $\mathcal{G}(t)$. Write collectively these n distributed estimators, we get the compact vector form as

$$\dot{w}(t) = -\gamma w(t) - L(t)z(t), \tag{5.3}$$

$$z(t) = w(t) + r(t). \tag{5.4}$$

Let $e_z(t)$ be the tracking error, we have $e_z(t) = z(t) - \bar{r}(t) \cdot \mathbb{1}$, where $\mathbb{1}$ denotes the column vector of n ones. Now, we are ready to state the convergence property of the dynamic average consensus filter (5.3) and (5.4).

Proposition 5.1.1 (Proportional dynamic consensus, *Theorem* 4 of [32])**.** *Let $L(t)$ be a piecewise continuous Laplacian of balanced graphs and $\Pi \in \mathbb{R}^{n \times n}$ be the projec-*

tion matrix $\Pi = I - \frac{\mathbb{1}\cdot\mathbb{1}^T}{n}$. *Suppose there exist* $\varepsilon \in \mathbb{R}$, *such that* $\Pi(L + L^T)\Pi \geq 2\varepsilon\Pi$ *for all* $t \geq t_0$. *Additionally, suppose we have non-negative parameter* γ, μ, *and absolutely continuous input function* $r(t)$ *satisfying* $\gamma > -\varepsilon$ *and* $\|\gamma r(t) + \dot{r}(t)\| \leq \mu$ *for almost all* $t \geq t_0$, *then the dynamic consensus filter* (5.3) *and* (5.4) *can track* $\bar{r}(t)$ *with tracking error* $e_z(t)$ *satisfying*

$$\|e_z(t)\| \leq \frac{1}{\sqrt{n}}|\mathbb{1}^T w(t_0)|e^{-\gamma(t-t_0)} + |\Pi z(t_0)|e^{(\gamma+\varepsilon)(t-t_0)} + \frac{\mu}{\gamma+\epsilon} \tag{5.5}$$

for all $t \geq t_0$.

5.2 Dynamic Max and Min Consensus

Again, suppose each agent $i \in \{1, \ldots, n\}$ maintains a time varying function $r_i(t)$. The dynamic max consensus is the problem of tracking the dynamic maximum of the r_i, i.e., $\max_i r_i(t)$, while dynamic min consensus tracks the minimum of the r_i, i.e., $\min_i r_i(t)$.

We begin with static case. The following static max and min consensus filters in continuous time are proposed in [34]

$$\dot{y}_i(t) = \mathrm{sgn}_+(\sum_{j=1}^{n} a_{ij}(y_j - y_i)), \tag{5.6}$$

$$\dot{y}_i(t) = \mathrm{sgn}_-(\sum_{j=1}^{n} a_{ij}(y_j - y_i)), \tag{5.7}$$

where $\mathrm{sgn}_+, \mathrm{sgn}_- : \mathbb{R} \to \mathbb{R}$ are defined as

$$\mathrm{sgn}_+(x) = \begin{cases} 0, & if \;\; x \leq 0 \\ 1, & if \;\; x > 0 \end{cases}, \qquad \mathrm{sgn}_-(x) = \begin{cases} 0, & if \;\; x \geq 0 \\ -1, & if \;\; x < 0 \end{cases}. \tag{5.8}$$

Note that the right-hand side of (5.6) is discontinuous, we understand its solution in the Filippov sense. We review the convergence property of these two filters as the following proposition.

Proposition 5.2.1 (Static Max and Min Consensus, *Propostion* 17 of [34])**.** *Let $\mathcal{G}$ be a strongly connected weighted digraph. Then, the coordination algorithm* (5.6) *(respectively,the coordination algorithm* (5.7)*) is out-distributed over $\mathcal{G}$ and asymptotically achieves max consensus (respectively, min consensus) in finite time.*

The max-consensus algorithm (5.6) is valid only for static input. In practice and research, from time to time, a group of agents needs to reach max-consensus distributedly of some interested quantities which are changing dynamically. Inspired by the proportional dynamic average consensus estimator (5.3) and (5.4) and the static max-consensus protocol (5.6), we propose the following dynamic max-consensus estimator (DMCE), for each agent $i \in \{1, \dots, n\}$

$$\begin{aligned} \dot{v}_i(t) = k_1 \operatorname{sgn}_+(\sum_{j=1}^{n} a_{ij}(t)[y_j(t) - y_i(t)]) \\ + k_2 v_i(t) \operatorname{sgn}_-(\sum_{j=1}^{n} a_{ij}(t)[y_j(t) - y_i(t)]), \end{aligned} \tag{5.9}$$

$$y_i(t) = v_i(t) + r_i(t). \tag{5.10}$$

where $k_1 \in \mathbb{R}_{>0}$ and $k_2 \in \mathbb{R}_{\geq 0}$ are proportional coefficients controlling the evolution speed of the flow, $r_i(t)$ is the input signal of agent i, output $y_i(t)$ is the estimation of $max_i r_i(t)$ by agent i. It is easy to see that when $r_i(t)$ is static with respect to $t \in \mathbb{R}$ for all $i \in \{1, \dots, n\}$, by letting $k_1 = 1$ and $k_2 = 0$, the proposed dynamic max-consensus estimator (5.9) and (5.10) degenerates to the static max-consensus estimator (5.6).

The mathematical analysis of the stability and convergence properties of the dynamic max-consensus estimator (5.9) and (5.10) is, so far, still our future work. We will verify the effectiveness of the proposed dynamic max-consensus estimator via simulations in the remaining part of this section.

5.2.1 Simulations

In the following simulations, we have a group of $n = 8$ agents. Each agent is assigned a unique ID $i \in \{1, \ldots, 8\}$. For each simulation, the algorithms are implemented in `Matlab` as a single centralized program. In the following simulations, we will use two undirected communication graphs $\mathcal{G}_1$ and $\mathcal{G}_2$ shown in Figure 5.1. The Laplacian $L(\mathcal{G}_1)$ and $L(\mathcal{G}_2)$ of $\mathcal{G}_1$ and $\mathcal{G}_2$ are, respectively,

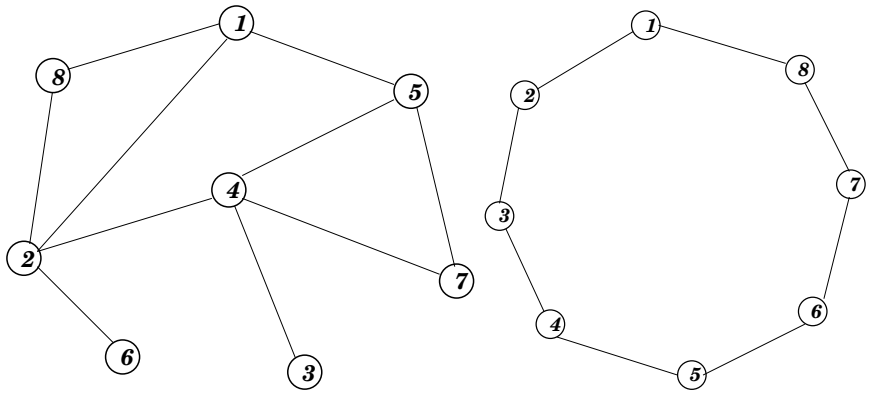

Figure 5.1: Two undirected communication graphs $\mathcal{G}_1$ (left) and $\mathcal{G}_2$ (right) both with 8 vertices, and all the edges have the same weight 1.

$$L(\mathcal{G}_1) = \begin{bmatrix} 3 & -1 & 0 & 0 & -1 & 0 & 0 & -1 \\ -1 & 4 & 0 & -1 & 0 & -1 & 0 & -1 \\ 0 & 0 & 1 & -1 & 0 & 0 & 0 & 0 \\ 0 & -1 & -1 & 4 & -1 & 0 & -1 & 0 \\ -1 & 0 & 0 & -1 & 3 & 0 & -1 & 0 \\ 0 & -1 & 0 & 0 & 0 & 1 & 0 & 0 \\ 0 & 0 & 0 & -1 & -1 & 0 & 2 & 0 \\ -1 & -1 & 0 & 0 & 0 & 0 & 0 & 2 \end{bmatrix},$$

$$L(\mathcal{G}_2) = \begin{bmatrix} 2 & -1 & 0 & 0 & 0 & 0 & 0 & -1 \\ -1 & 2 & -1 & 0 & 0 & 0 & 0 & 0 \\ 0 & -1 & 2 & -1 & 0 & 0 & 0 & 0 \\ 0 & 0 & -1 & 2 & -1 & 0 & 0 & 0 \\ 0 & 0 & 0 & -1 & 2 & -1 & 0 & 0 \\ 0 & 0 & 0 & 0 & -1 & 2 & -1 & 0 \\ 0 & 0 & 0 & 0 & 0 & -1 & 2 & -1 \\ -1 & 0 & 0 & 0 & 0 & 0 & -1 & 2 \end{bmatrix}.$$

Static inputs with fixed communication graph $\mathcal{G}_1$

Suppose each agent i maintains a constant measurement $r_i(t) = i$, for all $i \in \{1, \ldots, 8\}, t \in \mathbb{R}$. These 8 agents have a fixed undirected communication graph $\mathcal{G}_1$ shown in Figure 5.1. Since all the inputs of the group of agents are constant, we set the DMCE parameter $k_2 = 0$. Then, we have only tunable parameter k_1 left. However, when $k_2 = 0$, k_1 only controls the evolution speed. Not other properties of the estimator will be changed other than the evolution speed, when k_1 changes. In our simulation, we simply let $k_1 = 1$. Figure 5.2

shows the tracking performance. From the figures, we see the group of agents do reach max consensus.

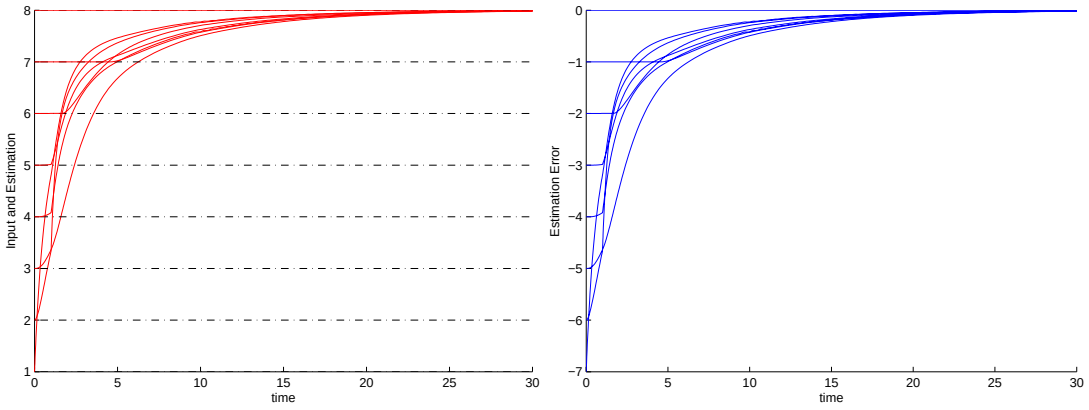

Figure 5.2: Max tracking with static inputs and fixed communication graph $\mathcal{G}_1$: on the left, estimation outputs (red solid line) and agents inputs (black dash-dotted line); on the right, estimation error.

Static inputs with switching communication graphs $\mathcal{G}_1$ and $\mathcal{G}_2$

In this part, we still suppose each of the 8 agents maintains a constant measurement $r_i(t) = i$. But the communication graphs are switching between $\mathcal{G}_1$ and $\mathcal{G}_2$ at every second with initial communication graph $\mathcal{G}_1$. Set the DMCE parameters as $k_1 = 1, k_2 = 0$. The estimation performance is shown in Figure 5.3.

Dynamic inputs with fixed communication graph $\mathcal{G}_1$

For the simulations in this section, the inputs of agents are not static any more. For any $t \in \mathbb{R}$, suppose each odd-numbered agent i has dynamic input

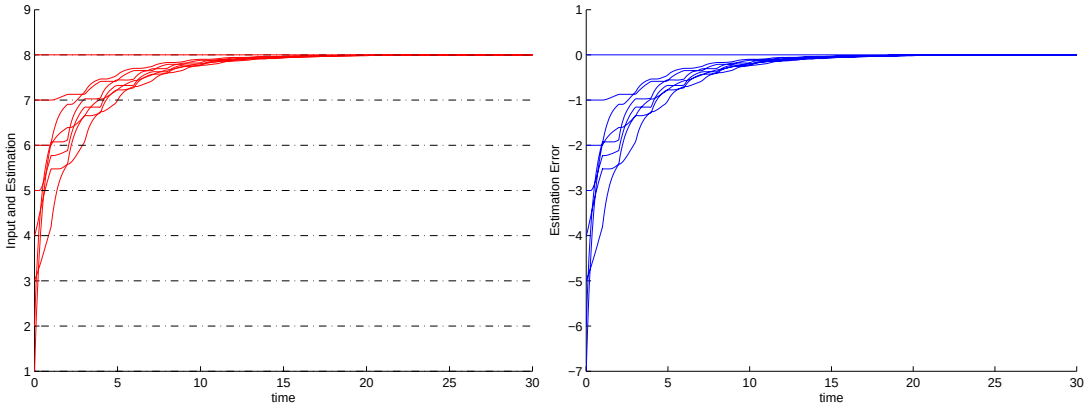

Figure 5.3: Max tracking with static inputs and switching communication graphs $\mathcal{G}_1$ and $\mathcal{G}_2$: on the left, estimation outputs (red solid line) and agents inputs (black dash-dotted line); on the right, estimation error.

$r_i(t) = \sin(\frac{i+1}{2} \cdot t)$, for $i \in \{1, 3, 5, 7\}$; while each even-numbered agent i has dynamic input $r_i(t) = \cos(\frac{i}{2} \cdot t)$, for $i \in \{2, 4, 6, 8\}$. We first simulate the DMCE with parameters $k_1 = 1$ and $k_2 = 0$, which is actually a static max consensus estimator. From the simulation results, shown in Figure 5.4, we see that the static max consensus estimator can not track the dynamic maximum of the network $\mathcal{G}_1$ successfully.

Let $k_1 = 1$ and $k_2 = 1$, the resulting estimator is not static max consensus estimator anymore. Figure 5.5 shows the tracking performance which is better than that in Figure 5.4. But the tracking errors are still too big, because the evolution speed of the dynamic max consensus estimator is relatively low compared with that of the dynamic inputs.

Set the parameters as $k_1 = 50$ and $k_2 = 10$, then we get a relatively high speed dynamic max consensus estimator compared to the dynamic inputs assigned in the beginning of the section. Figure 5.6 shows the improved tracking

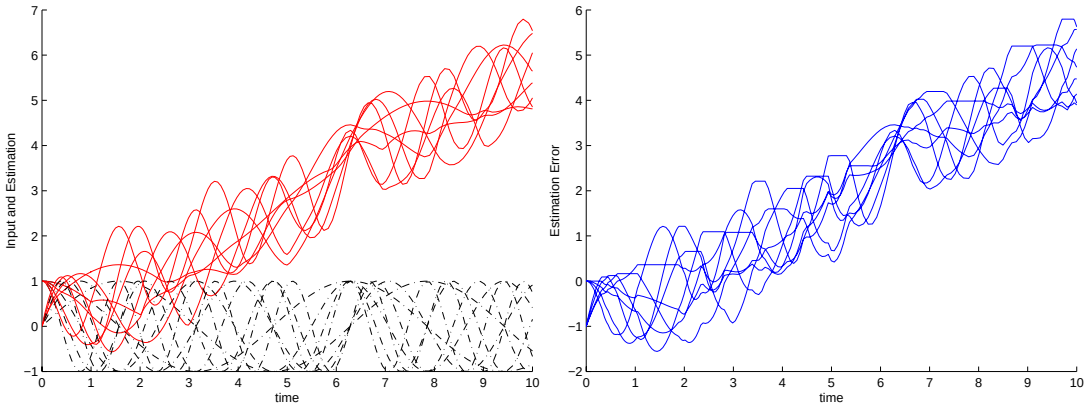

Figure 5.4: Track the dynamic maximum of network $\mathcal{G}_1$ using static max consensus estimator: on the left, estimation outputs (red solid line) and agents inputs (black dash-dotted line); on the right, estimation error.

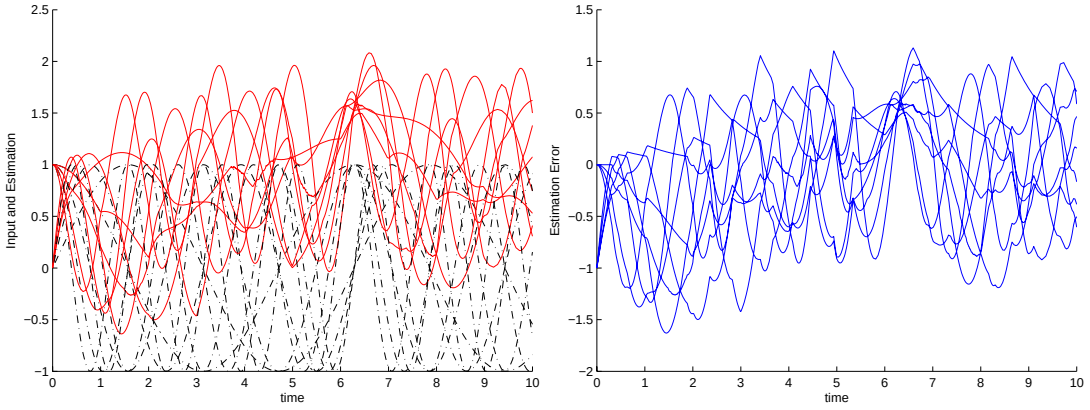

Figure 5.5: Track the dynamic maximum of network $\mathcal{G}_1$ using low speed dynamic max consensus estimator (DMCE): on the left, estimation outputs (red solid line) and agents inputs (black dash-dotted line); on the right, estimation error.

performance, which is much better than that in Figure 5.5. Figure 5.7 shows the tracking performance of the dynamic max consensus estimator with another set of dynamic inputs.

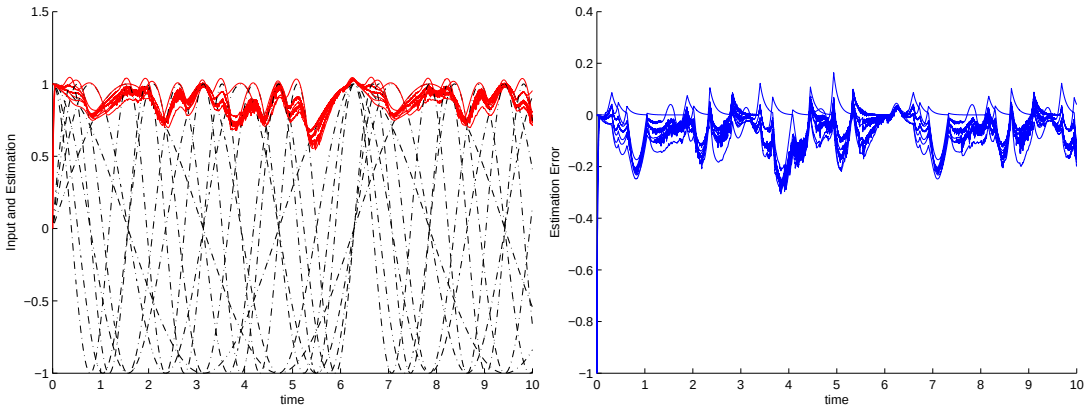

Figure 5.6: Track the dynamic maximum of network $\mathcal{G}_1$ using high speed dynamic max consensus estimator (DMCE): on the left, estimation outputs (red solid line) and agents inputs (black dash-dotted line); on the right, estimation error.

Dynamic inputs with switching communication graphs $\mathcal{G}_1$ and $\mathcal{G}_2$

Suppose the group of agents have the same inputs as in last section, but with switching communication graphs. The communication graphs are switching between $\mathcal{G}_1$ and $\mathcal{G}_2$ at every second with initial communication graph $\mathcal{G}_1$. The simulation results shown in Figure 5.8 are not significantly different than those shown in Figure 5.6.

The simulation results shown in Figure 5.2, 5.3, 5.6, 5.7 and 5.8 verify in part the effectiveness of the proposed dynamic max-consensus estimator (5.9)

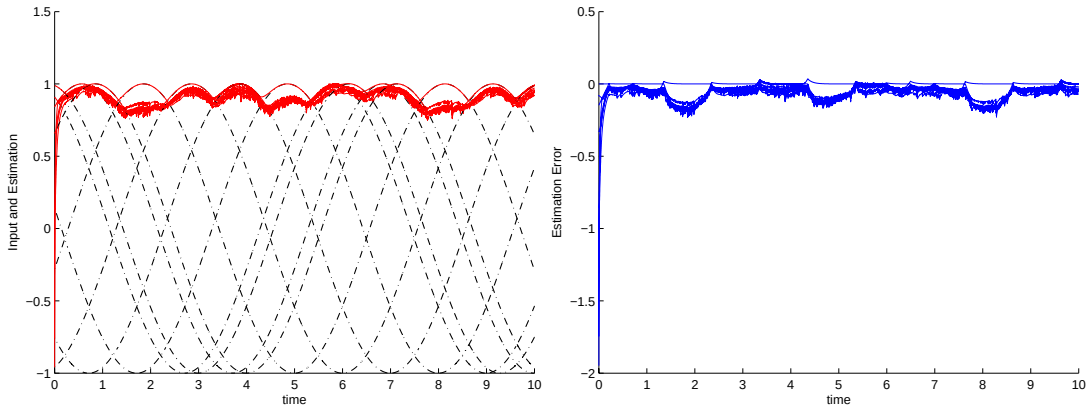

Figure 5.7: Track the dynamic maximum of network $\mathcal{G}_1$, with another set of inputs, using dynamic max consensus estimator (DMCE): on the left, estimation outputs (red solid line) and agents inputs (black dash-dotted line); on the right, estimation error.

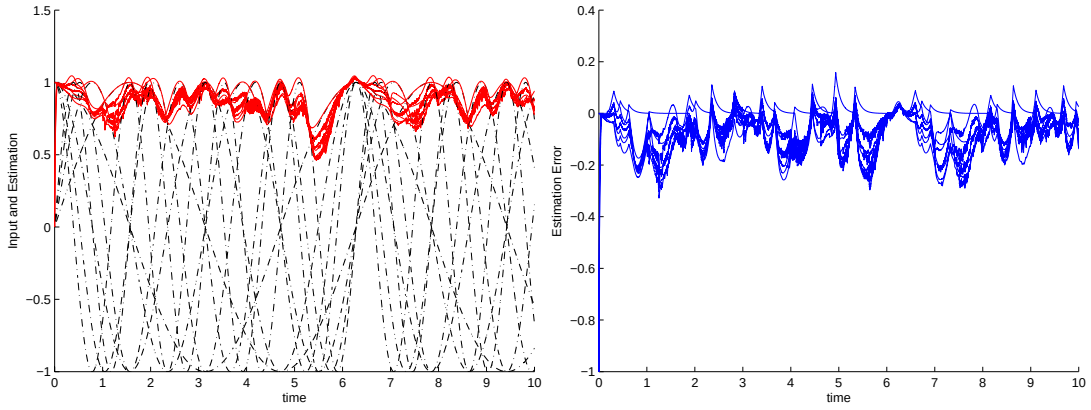

Figure 5.8: Track the dynamic maximum of a network of 8 agents with switching communication graphs $\mathcal{G}_1$ and $\mathcal{G}_2$ using dynamic max consensus estimator (DMCE): on the left, estimation outputs (red solid line) and agents inputs (black dash-dotted line); on the right, estimation error.

and (5.10). We will use this estimator to track the dynamic maximum of the measurements of a distributed sensor network in next chapter.

Finally, we mention that a dynamic minimum consensus problem can always be easily transformed into a dynamic maximum consensus problem and be solved using maximum consensus estimator, since

$$\min_i f_i = -\max_i(-f_i),$$

for any functions f_i.

Chapter 6

Global Optimization of Coverage Control

We have introduced the concept of distributed coverage control in both continuous space and discrete space in Chapter 4, where we also presented a class of gradient descent algorithms for optimal coverage. These coverage algorithms were proved to be adaptive, distributed and verifiably correct. One limitation of these algorithms is that they can only achieve local optima, other than global optima. To improve the performance of the mobile sensing network even more, we need to design control algorithm which can optimize the coverage performance *globally*.

In Section 6.1, we introduce a deterministic global optimization scheme named Terminal Repeller Unconstrained Subenergy Tunneling (TRUST); In Section 6.2, we discuss in detail our distributed estimation and control approach to solve global optimal coverage problem; Numerical simulation re-

sults are reported in Section 6.3.

6.1 Preliminaries on global optimization

Many engineering applications can be formulated as nonlinear function optimization problems in which the function to be optimized possesses many local minima in the parameter region of interest. The problem of designing algorithms that can distinguish between the global minimum and the numerous local minima is known as the global optimization. The primary difficulty in solving global optimization problems stems from the fact that the global extremum of a real function is, despite its name, a local property [35]. The existing approaches can be largely classified as deterministic and probabilistic. A deterministic global optimization scheme named *Terminal Repeller Unconstrained Subenergy Tunneling (TRUST)* was proposed in [35]. The TRUST formulates optimizations as the solution of a deterministic dynamical system incorporating terminal repellers and a novel subenergy tunneling function to ensure escape from local minima in a fast, reliable and computationally efficient manner.

We start with global minimization problem, and keep in mind that maximization problem could be easily transformed to a minimization problem. Let $f(x) : \mathbb{R}^n \rightarrow \mathbb{R}$ be a lower semi-continuous objective function with a finite number of discontinuities. The goal of global minimization is to find x_{GM}, such that $f(x_{\text{GM}}) = \min\{f(x) \mid x \in \mathcal{D}\}$, where $\mathcal{D}$ is the domain of interest over which we are seeking the global minimum. The first concept of TRUST is the

sub-energy tunneling transformation defined as

$$E_{\text{sub}}(x, x^*) = \log \frac{1}{1 + e^{-(\hat{f}(x)+a)}}, \tag{6.1}$$

where $\hat{f}(x) = f(x) - f(x^*)$, parameter a is a constant that affects only the asymptotic behavior not the monotonicity of the transformation and x^* is a fixed value whose selection is discussed in detail in [35] and [36]. $E_{\text{sub}}(x, x^*)$ is a nonlinear monotonic transformation of $f(x)$ which preserves all properties relevant for optimization. Specifically speaking, $E_{\text{sub}}(x, x^*)$ has the same discontinunity and extremal points as $f(x)$ and the same relative ordering of the local and global minima. In addition, this transformation is designed to satisfy that (i) $E_{\text{sub}}(x, x^*)$ approaches to zero quickly for $\hat{f}(x) \geq 0$; and (ii) $E_{\text{sub}}(x, x^*)$ tends rapidly toward $\hat{f}(x)$ when $\hat{f}(x) < 0$.

The second concept of TRUST is terminal repellers which utilizes the finite escape time property of some specific unstable dynamical systems, such as $\dot{x} = x^{\frac{1}{3}}$ with $x \in \mathbb{R}$. Assembling both concepts, sub-energy tunneling and terminal repeller, together, we define the TRUST virtual objective function as

$$\begin{aligned} E(x, x^*) &= E_{\text{sub}}(x, x^*) + E_{\text{rep}}(x, x^*) \\ &= \log \frac{1}{1 + e^{-(\hat{f}(x)+a)}} - \frac{3}{4}\rho(x - x^*)^{\frac{4}{3}}\theta[\hat{f}(x)], \end{aligned} \tag{6.2}$$

where $\theta[x] \in \mathbb{R}^n$ with its ith element $(\theta[x])_i = \text{sgn}_+(x_i)$.[1] The parameter $\rho > 0$ quantifies the strength of the repeller. Application of gradient descent to $E(x, x^*)$ results in the dynamical system, for $i \in \{1, \ldots, n\}$,

$$\dot{x}_i = -\frac{\partial f(x)}{\partial x_i} \frac{1}{1 + e^{(\hat{f}(x)+a)}} + \rho(x_i - x_i^*)^{\frac{1}{3}}\theta[\hat{f}(x)]. \tag{6.3}$$

[1] Recall the definition of $\text{sgn}_+(\cdot)$ in equation (5.8).

The virtual objective function $E(x, x^*)$ transforms the current local minimum of $f(x)$ into a global maximum, but preserves all lower local minima. Thus, the gradient descent dynamics (6.3), initialized at a small perturbation from the local minimum of $f(x)$, will escape this critical point to a lower valley of $f(x)$ with a lower local minimum, resulting in a system that has a global descent property. This is the main idea of the TRUST method. An enhanced dynamical system

$$\dot{x}_i = -\frac{\partial f(x)}{\partial x_i}\frac{1}{1+e^{(\hat{f}(x)+a)}} + \rho\omega_i(x_i - x_i^*)^{\frac{1}{3}}\theta[\hat{f}(x)], \tag{6.4}$$

was presented in [36], where ω_i is defined as

$$\omega_i = \left|\frac{\partial f(x)}{\partial x_i}\right| / \max_i \left|\frac{\partial f(x)}{\partial x_i}\right|, \quad i \in \{1, \ldots, n\}.$$

The term ω_i is introduced to ensure better convergence to a global minimum.

6.2 A distributed Estimation-and-Control approach to optimize coverage control globally

We follow the distributed simultaneous estimation and control framework proposed in [37] to optimize coverage control globally. Our approach is based on TRUST method.

For easy reading, we use the same setup, assumption and notation as in Section 4.1, where our objective is to maximize multi-center functions $\mathcal{H}(P)$ and $\mathcal{H}_{\text{dscrt}}(P)$. Since the standard TRUST method introduced in previous section is stated in the form of solving global minimization problem, for clearness

and consistence with the TRUST approach, we define a new unified notation $\mathbb{H}$ as

$$\mathbb{H} = \begin{cases} -\mathcal{H}(P), & \text{for coverage in continuous space} \\ -\mathcal{H}_{\text{dscrt}}(P), & \text{for coverage in discrete space} \end{cases},$$

which transforms the original maximization problems to minimization problems and keeps the continunity and derivability unchanged.

Adopting the enhanced TRUST algorithm (6.4), we obtain the following coverage control law

$$u_i = -\frac{\partial \mathbb{H}}{\partial p_i} \frac{1}{1 + e^{\hat{\mathbb{H}} + a}} + \rho z_i \theta[\hat{\mathbb{H}}], \tag{6.5}$$

where $i \in \{1, \ldots, n\}$ and

$$\begin{aligned} z_i &= \begin{bmatrix} z_{i1} \\ z_{i2} \end{bmatrix} = \begin{bmatrix} \omega_{i1}(p_{i1} - p_{i1}^*)^{\frac{1}{3}} \\ \omega_{i2}(p_{i2} - p_{i2}^*)^{\frac{1}{3}}, \end{bmatrix}, \\ \omega_{ij} &= \left| \frac{\partial \mathbb{H}}{\partial p_{ij}}(P) \right| / \max_{l,m} \left| \frac{\partial \mathbb{H}}{\partial p_{lm}}(P) \right|, \quad j \in \{1, 2\}, \\ \hat{\mathbb{H}} &= \mathbb{H}(P) - \mathbb{H}(P^*). \end{aligned}$$

Unlike the orginal coverage control laws (4.4) and (4.5), control law 6.5 is not distributed any more, since $\hat{\mathbb{H}}(P)$ and z_i are not locally available to agent i. But still we can say that this control law only needs very limited global information of the system, only the overall system performance $\hat{\mathbb{H}}$ and the maximum element of the gradient flows $\left| \frac{\partial \mathbb{H}}{\partial p_{lm}} \right|$ are required. We use the estimation-and-control approach to solve this problem. More specifically, each agent i runs locally a dynamic average consensus estimator to estimate $\hat{\mathbb{H}}$, and a dynamic max-consensus estimator to estimate $\max \left| \frac{\partial \mathbb{H}}{\partial p_{lm}} \right|$.

Dynamic Average Consensus

We use dynamic average consensus filter (5.3) and (5.4) to estimate the coverage performance of the sensor networks $\mathbb{H}$. Each agent of the network implements the following estimator

$$\dot{w}_i(t) = k_{\mathrm{AC}} \sum_{j \neq i} a_{ij}(t)[z_j(t) - z_i(t)],$$
$$z_i(t) = w_i(t) + h_i(t).$$

where $h_i(t) \in \mathbb{R}$, the coverage performance of agent i, is the input of estimator, $z_i(t) \in \mathbb{R}$ is the decision variable, $w_i(t) \in \mathbb{R}$ is the internal state of the estimator, $a_{ij}(t)$ is the weight of the edge (i, j) of the communication graph, k_{AC} is a positive gain adjusting the convergence speed of the average consensus estimator. Then, agent i's estimation of $\mathbb{H}$ will be $n \cdot z_i$.

Dynamic Max Consensus

We use dynamic max consensus estimator (5.9) and (5.10) to estimate the maximum element of the gradient flows $\left|\frac{\partial \mathbb{H}}{\partial p_{lm}}\right|$. Each agent of the network implements the following estimator

$$\begin{aligned}\dot{v}_i(t) = k_1 \operatorname{sgn}_+(\sum_{j=1}^{n} a_{ij}(t)[y_j(t) - y_i(t)]) \\ + k_2 v_i(t) \operatorname{sgn}_-(\sum_{j=1}^{n} a_{ij}(t)[y_j(t) - y_i(t)]),\end{aligned} \tag{6.6}$$

$$y_i(t) = v_i(t) + r_i(t). \tag{6.7}$$

where $k_1 \in \mathbb{R}_{>0}$ and $k_2 \in \mathbb{R}_{\geq 0}$ are proportional coefficients controlling the evolution speed of the flow; $r_i(t)$ is the input signal of agent i, which satisfies

$$r_i = \max\{\left|\frac{\partial \mathbb{H}}{\partial p_{i1}}\right|, \left|\frac{\partial \mathbb{H}}{\partial p_{i2}}\right|\};$$

and output $y_i(t)$ is the estimation of $\max_j r_j(t)$ by agent i. Since

$$\max_{l,m} \left|\frac{\partial \mathbb{H}}{\partial p_{lm}}\right| = \max_j r_j(t),$$

so y_i is agent i's estimation of the maximum element of $\left|\frac{\partial \mathbb{H}}{\partial p_{lm}}\right|$.

6.3 Numerical simulations

We use the distributed estimation-and-control approach to optimize coverage globally in discrete space. In this simulation, we use a group of $n = 8$ agents to cover/surveil a polygon in $\mathbb{R}^2$ with 159 discrete target points. The simulation results shown in Figures 6.1, 6.2, 6.3 and 6.4 verify the effectiveness of the proposed approach..

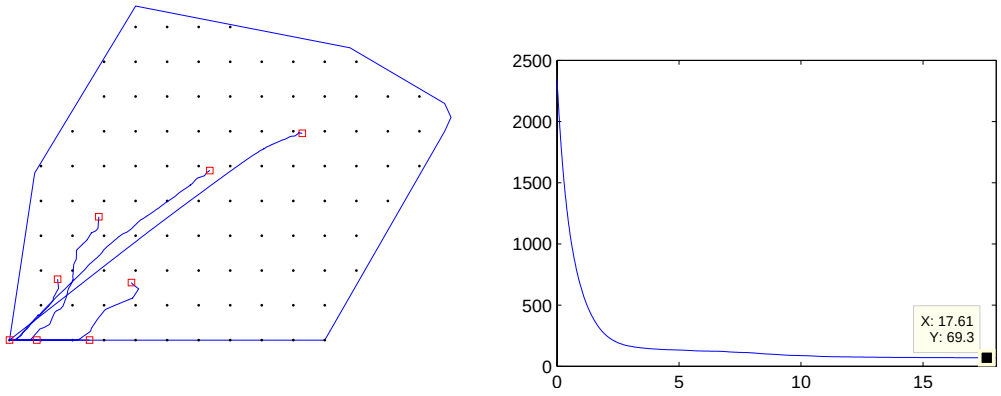

Figure 6.1: Agents start at the bottom left corner of the polygon and end at first local minimum with cost $\mathbb{H} = 69.3$: trajectories of agents (left), evolution of the cost $\mathbb{H}$ (right).

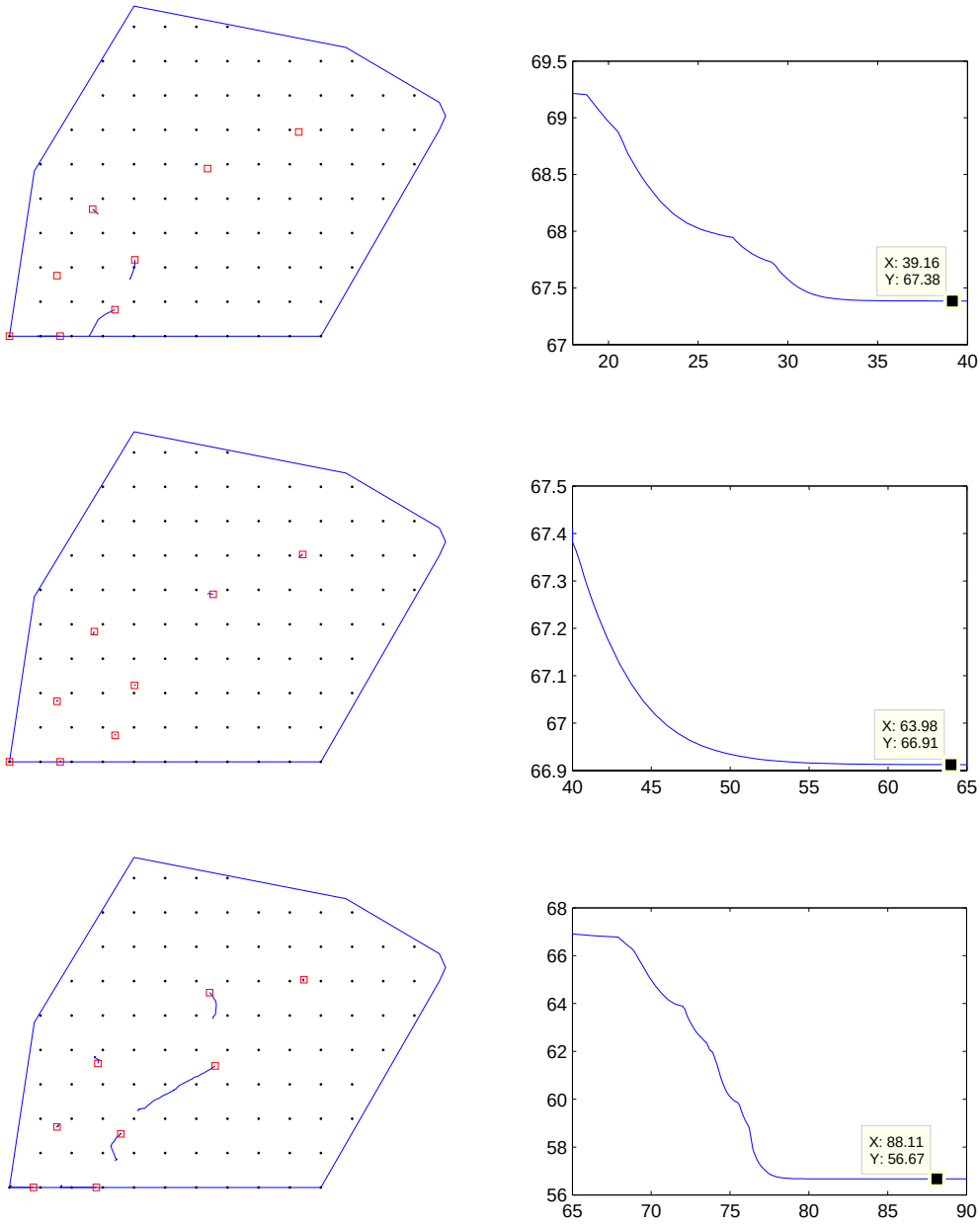

Figure 6.2: From up to down, agents start from previous local minima and end at new local minima with improving locally optimal cost $\mathbb{H}$, 67.38, 66.91, 56.67, respectively: trajectories of agents (left), evolution of the cost $\mathbb{H}$ (right).

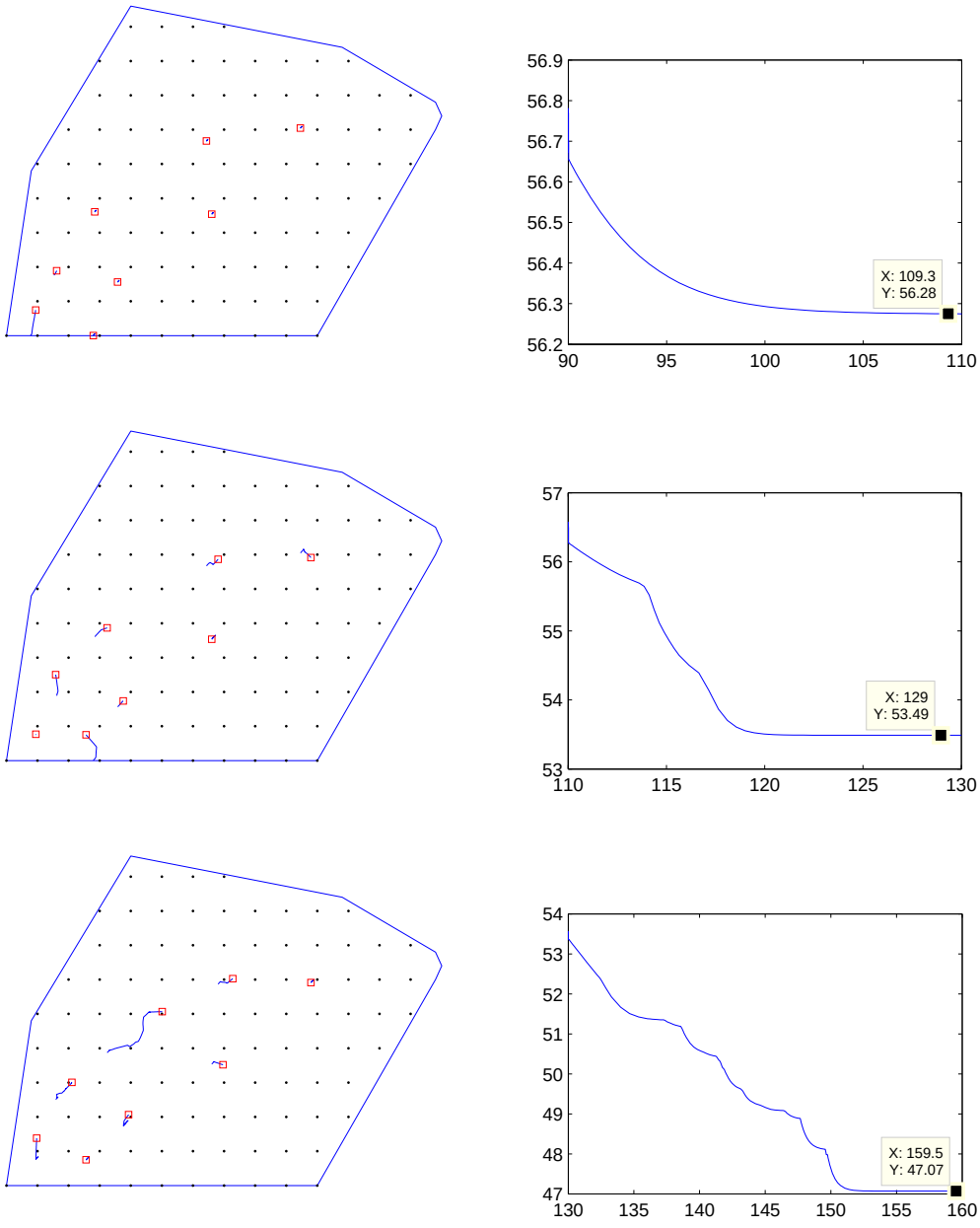

Figure 6.3: From up to down, agents start from previous local minima and end at new local minima with improving locally optimal cost $\mathbb{H}$, 56.28, 53.49, 47.07, respectively: trajectories of agents (left), evolution of the cost $\mathbb{H}$ (right).

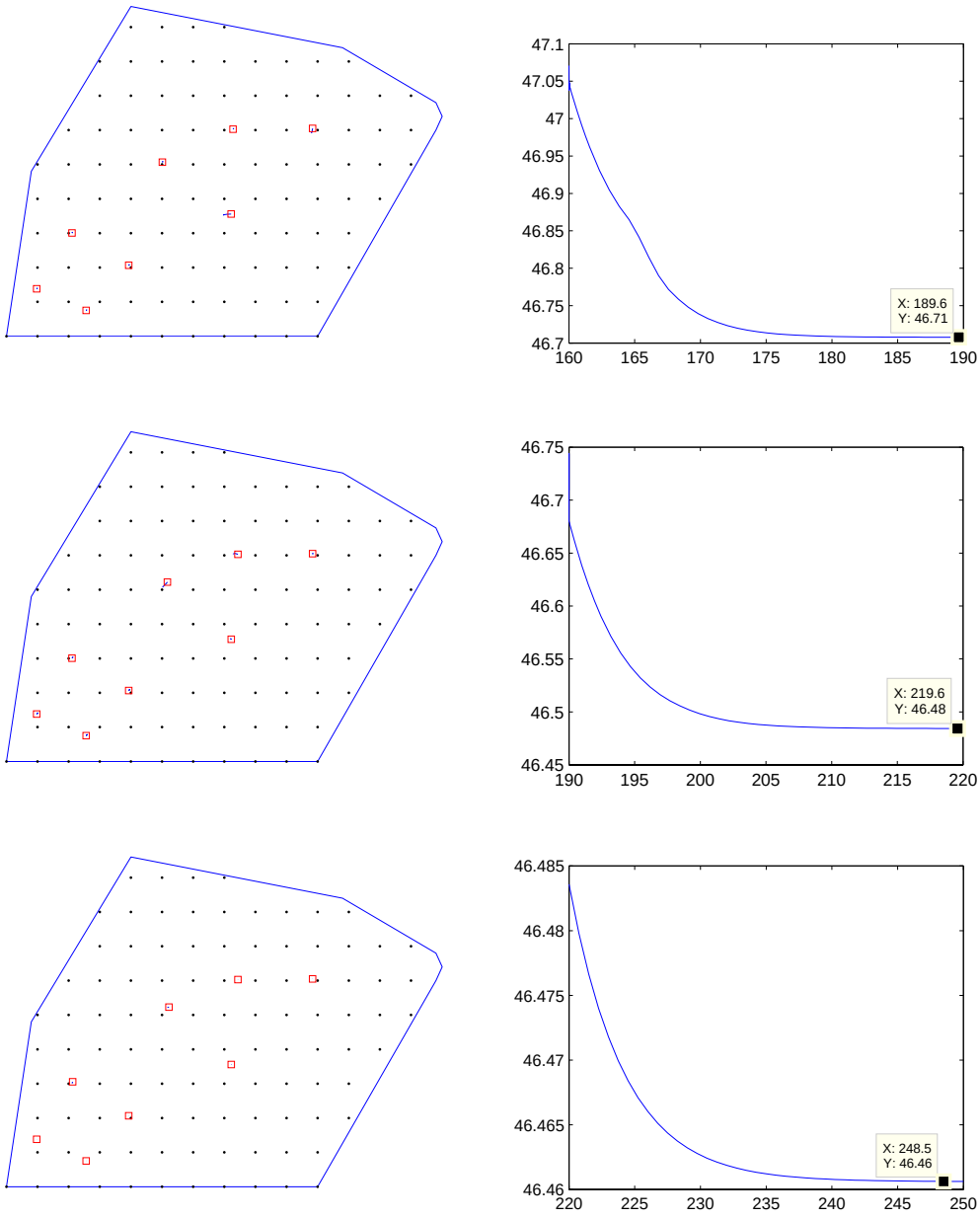

Figure 6.4: From up to down, agents start from previous local minima and end at new local minima with improving locally optimal cost $\mathbb{H}$, 46.71, 46.48, 46.46, respectively: trajectories of agents (left), evolution of the cost $\mathbb{H}$ (right). The last local minimum is the global minimum found by our distributed estimation-and-control approach.

Chapter 7

Conclusions

In Chapter 3, we have studied averaging protocols over fixed and controlled-switching acyclic digraphs, and characterized their asymptotic convergence properties. In Chapter 4, we have discussed continuous and discrete multi-center locational optimization functions, and distributed control laws that optimize them. The main result of Chapter 3 and Chapter 4 shows how these two sets of problems are intimately related: discrete coverage control laws are indeed averaging protocols over acyclic digraphs. As a consequence of our analysis, it may be argued that the coverage control problem and the consensus problem are both special cases of a general class of distributed optimization problems.

In Chapter 5, we have reviewed the results on dynamic average consensus problems available on the literature and proposed a dynamic max/min consensus estimator and verified its effectiveness by simulations. The results of Chapter 5 on dynamic consensus serve as a basis for Chapter 6, where we

proposed a distributed estimation and control approach to optimize coverage control globally. We have simulated the approach numerically for a discrete coverage problem and obtained improved results. It is our future work to analyze the stability and convergence properties of the estimators and control laws proposed in Chapter 5 and Chapter 6.

Bibliography

[1] J. Cortés, S. Martínez, T. Karatas, and F. Bullo, "Coverage control for mobile sensing networks," *IEEE Transactions on Robotics and Automation*, vol. 20, no. 2, pp. 243–255, 2004.

[2] A. Okabe, B. Boots, K. Sugihara, and S. N. Chiu, *Spatial Tessellations: Concepts and Applications of Voronoi Diagrams*. Wiley Series in Probability and Statistics, New York: John Wiley, 2 ed., 2000.

[3] R. Diestel, *Graph Theory*, vol. 173 of *Graduate Texts in Mathematics*. New York: Springer Verlag, 2 ed., 2000.

[4] A. F. Filippov, *Differential Equations with Discontinuous Righthand Sides*, vol. 18 of *Mathematics and Its Applications*. Dordrecht, The Netherlands: Kluwer Academic Publishers, 1988.

[5] F. H. Clarke, *Optimization and Nonsmooth Analysis*. Canadian Mathematical Society Series of Monographs and Advanced Texts, John Wiley, 1983.

[6] A. Bacciotti and L. Rosier, *Liapunov Functions and Stability in Control Theory*. New York, NY: Springer Verlag, 2 ed., 2005.

[7] R. Olfati-Saber and R. M. Murray, "Consensus problems in networks of agents with switching topology and time-delays," *IEEE Transactions on Automatic Control*, vol. 49, no. 9, pp. 1520–1533, 2004.

[8] W. Ren, R. W. Beard, and E. M. Atkins, "A survey of consensus problems in multi-agent coordination," in *American Control Conference*, (Portland, OR), pp. 1859–1864, June 2005.

[9] J. Cortés, "Discontinuous dynamical systems - a tutorial on notions of solutions, nonsmooth analysis, and stability," *IEEE Control Systems Magazine*, Jan. 2007. submitted.

[10] B. Paden and S. S. Sastry, "A calculus for computing Filippov's differential inclusion with application to the variable structure control of robot manipulators," *IEEE Transactions on Circuits and Systems*, vol. 34, no. 1, pp. 73–82, 1987.

[11] A. Bacciotti and F. Ceragioli, "Stability and stabilization of discontinuous systems and nonsmooth Lyapunov functions," *ESAIM. Control, Optimisation & Calculus of Variations*, vol. 4, pp. 361–376, 1999.

[12] D. Shevitz and B. Paden, "Lyapunov stability theory of nonsmooth systems," *IEEE Transactions on Automatic Control*, vol. 39, no. 9, pp. 1910–1914, 1994.

[13] D. Bauso, L. Giarré, and R. Pesenti, "Distributed consensus in networks of dynamic agents," in *IEEE Conf. on Decision and Control and European Control Conference*, (Seville, Spain), pp. 7054–7059, 2005.

[14] J. Cortés, "Analysis and design of distributed algorithms for χ-consensus," in *IEEE Conf. on Decision and Control*, (San Diego, CA), pp. 3363–3368, Dec. 2006.

[15] W. Ren and R. W. Beard, "Consensus seeking in multi-agent systems under dynamically changing interaction topologies," *IEEE Transactions on Automatic Control*, vol. 50, no. 5, pp. 655–661, 2005.

[16] J. N. Tsitsiklis, D. P. Bertsekas, and M. Athans, "Distributed asynchronous deterministic and stochastic gradient optimization algorithms," *IEEE Transactions on Automatic Control*, vol. 31, no. 9, pp. 803–812, 1986.

[17] A. Jadbabaie, J. Lin, and A. S. Morse, "Coordination of groups of mobile autonomous agents using nearest neighbor rules," *IEEE Transactions on Automatic Control*, vol. 48, no. 6, pp. 988–1001, 2003.

[18] L. Moreau, "Stability of multiagent systems with time-dependent communication links," *IEEE Transactions on Automatic Control*, vol. 50, no. 2, pp. 169–182, 2005.

[19] D. Angeli and P.-A. Bliman, "Stability of leaderless discrete-time multi-agent systems," *Mathematics of Control, Signals and Systems*, vol. 18, no. 4, pp. 293–322, 2006.

[20] V. D. Blondel, J. M. Hendrickx, A. Olshevsky, and J. N. Tsitsiklis, "Convergence in multiagent coordination, consensus, and flocking," in *IEEE Conf. on Decision and Control and European Control Conference*, (Seville, Spain), pp. 2996–3000, Dec. 2005.

[21] G. Ferrari-Trecate, A. Buffa, and M. Gati, "Analysis of coordination in multi-agent systems through partial difference equations," *IEEE Transactions on Automatic Control*, vol. 51, no. 6, pp. 1058–1063, 2006.

[22] L. Xiao and S. Boyd, "Fast linear iterations for distributed averaging," *Systems & Control Letters*, vol. 53, pp. 65–78, 2004.

[23] S. Guattery and G. L. Miller, "Graph embeddings and Laplacian eigenvalues," *SIAM Journal on Matrix Analysis and Applications*, vol. 21, no. 3, pp. 703–723, 2000.

[24] T. Vicsek, A. Czirók, E. Ben-Jacob, I. Cohen, and O. Shochet, "Novel type of phase transition in a system of self-driven particles," *Physical Review Letters*, vol. 75, no. 6-7, pp. 1226–1229, 1995.

[25] A. Bensoussan and J.-L. Menaldi, "Difference equations on weighted graphs," *Journal of Convex Analysis*, vol. 12, no. 1, pp. 13–44, 2005.

[26] R. Olfati-Saber, J. A. Fax, and R. M. Murray, "Consensus and cooperation in multi-agent networked systems," *Proceedings of the IEEE*, vol. 45, no. 1, pp. 215–233, 2007.

[27] W. Ren, R. W. Beard, and T. W. McLain, "Coordination variables and consensus building in multiple vehicle systems," in *Cooperative Control* (V. Kumar, N. E. Leonard, and A. S. Morse, eds.), vol. 309 of *Lecture Notes in Control and Information Sciences*, pp. 171–188, Springer Verlag, 2004.

[28] Z. Drezner, ed., *Facility Location: A Survey of Applications and Methods*. Springer Series in Operations Research, New York: Springer Verlag, 1995.

[29] Q. Du, V. Faber, and M. Gunzburger, "Centroidal Voronoi tessellations: Applications and algorithms," *SIAM Review*, vol. 41, no. 4, pp. 637–676, 1999.

[30] J. Cortés, S. Martínez, and F. Bullo, "Spatially-distributed coverage optimization and control with limited-range interactions," *ESAIM. Control, Optimisation & Calculus of Variations*, vol. 11, pp. 691–719, 2005.

[31] J. Cortés and F. Bullo, "Coordination and geometric optimization via distributed dynamical systems," *SIAM Journal on Control and Optimization*, vol. 44, no. 5, pp. 1543–1574, 2005.

[32] R. A. Freeman, P. Yang, and K. M. Lynch, "Stability and convergence properties of dynamic average consensus estimators," in *IEEE Conf. on Decision and Control*, (San Diego, CA), pp. 398–403, Dec. 2006.

[33] D. P. Spanos, R. Olfati-Saber, and R. M. Murray, "Dynamic consensus for mobile networks," in *IFAC World Congress*, (Prague, Czech), jul 2005.

[34] J. Cortés, "Distributed algorithms for reaching consensus on general functions," *Automatica*, 2007. To appear.

[35] J. Barhen, V. Protopopescu, and D. Reister, "TRUST: a deterministic algorithm for global optimization," *Science*, vol. 276, pp. 1094–1097, May 1997.

[36] J. Barhen and V. Protopopescu, "Generalized trust algorithms for global optimization," in *State of the art in global optimization* (C. A. Floudas and P. M. Pardalos, eds.), vol. 7 of *Nonconvex optimization and its applications*, pp. 163–180, The Netherlands: Kluwer Academic Publishers, 196.

[37] P. Yang, R. A. Freeman, and K. M. Lynch, "Multi-agent coordination by decentralized estimation and control," *IEEE Transactions on Automatic Control*, 2006. Submitted.